A Review of African Easterly Waves: Formation, Growth, Structure, and Evolution

KELLY M. NÚÑEZ OCASIO,[a] QUINTON A. LAWTON,[b] ALAN BRAMMER,[c] EMILY BERCOS-HICKEY,[d] STELLA BOURDIN,[e,f] XIANGBO FENG,[g] AND JULIANE SCHWENDIKE[h]

[a] Department of Atmospheric Sciences, Texas A&M University, College Station, Texas
[b] NSF National Center for Atmospheric Research, Boulder, Colorado
[c] Cooperative Institute for Research in the Atmosphere, Colorado State University, Fort Collins, Colorado
[d] Climate and Ecosystem Sciences Division, Lawrence Berkeley National Laboratory, Berkeley, California
[e] Atmospheric, Oceanic and Planetary Physics, Department of Physics, University of Oxford, Oxford, United Kingdom
[f] Laboratoire de Météorologie Dynamique, École Polytechnique, Palaiseau, France
[g] National Centre for Atmospheric Science and Department of Meteorology, University of Reading, Reading, United Kingdom
[h] Institute for Climate and Atmospheric Science, School of Earth and Environment, University of Leeds, Leeds, United Kingdom

(Manuscript received 28 September 2025, in final form 26 February 2026, accepted 17 April 2026)

ABSTRACT: This paper presents a comprehensive review of African easterly waves (AEWs), which are cold-core, synoptic-scale disturbances that exhibit horizontal and vertical tilts, often westward (eastward) with height above (below) the African easterly jet (AEJ), consistent with their baroclinic–barotropic nature. AEWs typically have wavelengths of 2000–6000 km, periods of 3–5 days, and westward propagation speeds of 7–9 m s^{-1}. Although AEWs have been observed and linked to African rainfall variability and tropical cyclone (TC) precursors since the 1930s, the theoretical framework explaining their formation was developed over 50 years ago and continues to inform our understanding of their energetics and evolution. The initiation and the horizontal and vertical structures of AEWs are reviewed, as these characteristics, especially their convective nature, can indicate wave growth and, in some cases, TC genesis. While TC genesis is not the focus of this paper, it emerges in AEW evolution. Perspectives differ on whether AEJ instabilities or upscale convective forcing is more critical to AEW growth, though both views have been shaped by available data and modeling tools. We argue the mechanisms are complementary. We include a summary of AEW tracking methods to assist future researchers in selecting approaches. Notably, most trackers tend to be more sensitive to southern-track AEWs than northern-track AEWs, likely due to stronger convective signals in the former systems. Finally, we discuss how AEW activity may respond to climate change, with evidence of a strengthening and poleward shift since 1980. The advent of convection-permitting models and machine learning tools offers potential for new insights into AEW growth and evolution.

KEYWORDS: Africa; Atlantic Ocean; Rossby waves; Monsoons; Atmospheric waves; Tropical variability

1. A historical glimpse into the early accounts of African easterly waves

The first descriptions of disturbances originating from Africa were made by Piersig (1936) and Regula (1936), using surface data from the eastern Atlantic and western Africa. They suggested that these disturbances might be responsible for many of the tropical cyclones (TCs) observed over the Atlantic and the Caribbean. A publication by Hubert (1939) identified a similar disturbance as the origin of the 1938 New England Hurricane. Soon after, in 1940, forecaster Gordon Dunn used the term "isallobaric waves" to describe features seen on isobar maps, which he linked to inversion layer breakdowns and TC development (Dunn 1940; NOAA 2015). Early hypotheses about their origins focused on trade winds, Earth's rotation, and interactions between the northeasterly trades and the West African monsoon (WAM). The term "African easterly waves" (AEWs) was later coined by Riehl (1945), who identified their characteristic "inverted trough" structure. In 1964, Riehl confirmed these findings by flying into an AEW over the Caribbean aboard a U.S. Weather Bureau's research aircraft (Riehl 1945).

With the advent of satellite observations in the 1960s and increased field campaigns, researchers began consistently tracking AEWs. Simpson et al. (1968) tracked over 60 disturbances using satellite imagery and surface data near the African coast. These disturbances shared common temporal and spatial scales, with a spectral peak of 3–5 days, wavelengths generally extending 2000–4000 km, and speeds of 7–9 m s^{-1} (Burpee 1972, 1974; Reed et al. 1977). These studies highlighted their substantial rainfall impacts over Africa and downstream regions, as many AEWs eventually developed into TCs, emphasizing the importance of understanding their formation and further development. Prior to this, only a few had been identified as hurricane precursors (Erickson 1963; Arnold 1966; Dunn 1962). Observations also revealed AEWs' role in transporting the hot, dry, and dusty Saharan air layer (SAL) from North Africa during the boreal summer, which aligns with peak AEW activity (e.g., Delany et al. 1967; Prospero 1968; Prospero and Carlson 1970; Burpee 1972).

Denotes content that is immediately available upon publication as open access.

Corresponding author: Kelly M. Núñez Ocasio, knunez.ocasio@tamu.edu

DOI: 10.1175/JAS-D-25-0175.1

Research over the last two decades has highlighted the impacts of AEWs on rainfall variability and extremes over Africa. These waves have been found to modulate and organize convection, including mesoscale convective systems (MCSs), as they propagate across the African continent (e.g., Berry and Thorncroft 2005; Mekonnen et al. 2006; Kiladis et al. 2006; Janiga and Thorncroft 2016). They also have a dominant impact on the spatiotemporal variability of clouds and rainfall over much of the African Sahel (Fink and Reiner 2003; Lubis and Jacobi 2015). Notably, AEWs have been linked to MCS-driven extreme rainfall events, which may have profound socioeconomic impacts (Nicholls and Mohr 2010; Crétat et al. 2015; Lafore et al. 2017; Engel et al. 2017; Maranan et al. 2019; Salifou et al. 2026). As a result, recent work has sought to quantify the interannual modulation of these waves by large-scale drivers such as El Niño–Southern Oscillation (ENSO), showing that La Niña conditions typically enhance AEW activity and associated convection relative to El Niño years (Ruti and Dell'Aquila 2010; Spinks and Lin 2015; Lawton et al. 2025). This teleconnection is thought to exist due to the modulation of regional circulations and thereby vertical wind shear by ENSO (Lawton et al. 2025). Just as AEWs are impacted by phenomena on interannual time scales, they may also be sensitive to long-term and short-term changes in Earth's climate system, a topic of growing research interest (e.g., Bercos-Hickey et al. 2023; Núñez Ocasio and Dougherty 2024; Núñez Ocasio et al. 2025; Akinsanola et al. 2025). For example, recent work using kilometer-scale simulations has suggested that AEWs may become more intense, have more moisture, and produce more rainfall in future climates (Núñez Ocasio et al. 2025).

Today, AEWs are recognized as high-impact tropical weather systems. These systems are closely linked to convection and are capable of producing intense rainfall. They also contribute to subseasonal rainfall variability across Africa, serve as hurricane precursors, and transport Saharan dust either independently or in conjunction with convection (e.g., Carlson 1969b,a). Theoretical and empirical frameworks explaining their formation and evolution have developed rigorously since the earliest studies, and now, these frameworks form the foundation of our modern understanding of AEWs.

The goal of this article is to provide a comprehensive overview of AEW initiation and growth (section 2), structure (section 3), and tracking (section 4). We also review our current understanding of future changes to AEW activity and the AEW–African easterly jet (AEJ) system (section 5). We hope this article provides readers with a clearer view of the consensus and deeper understanding of AEWs, while also highlighting key knowledge gaps.

In section 6, we provide a summary, discuss current challenges in AEW research, and offer suggestions for future directions. Although not the primary focus of this review, the role of AEWs in tropical cyclogenesis is a recurring theme that naturally emerges throughout the review, particularly in sections 2 and 3, where we discuss how further growth of AEWs and the proper structural and convective characteristics can lead to genesis.

While several reviews exist on various forms of tropical variability, such as MCSs (e.g., Houze 2004), equatorial waves (e.g., Knippertz et al. 2022), the Madden–Julian oscillation (e.g., Zhang 2005), and TCs (e.g., Emanuel 2003), this is, to our knowledge, the first review focusing solely on AEWs as complex high-impact weather systems.

2. AEW initiation and growth

Understanding the initiation and growth of AEWs is fundamental to grasping their structure, evolution, and broader impacts. This section examines the dynamical and thermodynamical processes that give rise to AEWs and support their development across West Africa and into the Atlantic.

AEWs are defined as synoptic-scale, westward-propagating disturbances that move across sub-Saharan Africa in the boreal summer (Riehl 1945). This time of year is characterized by strong meridional thermal contrasts: A heat low develops in the Sahara Desert due to intense solar radiation, while equatorial regions to the south become even more cooler and moister with the onset of the WAM (Fig. 1). This contrast is further enhanced by the development of the Atlantic cold tongue in the equatorial waters of the Atlantic, produced by wind-driven Ekman transport (e.g., Okumura and Xie 2004). The resulting temperature gradient induces a midtropospheric thermal jet, known as the AEJ, which becomes a key dynamical feature in AEW initiation and maintenance; the jet variability is related to eddy fluxes (Arnold 1966; Carlson 1969b,a; Cornforth et al. 2017).

Building on the Charney–Stern criterion for jet instability (Charney and Stern 1962), Burpee (1972) proposed that AEWs derive energy from instability within the AEJ. These instabilities include a combination of dry barotropic and baroclinic processes, arising from horizontal and vertical wind shear, which are associated with a reversal in the meridional gradient of potential vorticity (PV) near the jet core. This framework provided a theoretical foundation for interpreting AEWs during the formation stages as a type of dry Rossby wave (Thorncroft and Hoskins 1994a,b; Thorncroft and Hodges 2001, hereafter TH01; Pytharoulis and Thorncroft 1999). Burpee (1972) advanced this theory using 5 years of surface and upper-air data from weather stations across Africa. Through spectral analysis of wind, temperature, humidity, geopotential height, and surface pressure, he identified a consistent AEW signal at 700 hPa—resembling an inverted trough wind pattern—further validating the AEJ instability hypothesis.

A major milestone in observational research came with the 1974 Global Atmospheric Research Program (GARP) Atlantic Tropical Experiment (GATE), which used satellite, aircraft, and ground-based data to study synoptic and mesoscale systems over Africa and the tropical Atlantic (Reed et al. 1977; Norquist et al. 1977; Jenney et al. 2025). GATE was pivotal in advancing understanding of convection–AEW interactions, African MCSs, and the Atlantic intertropical convergence zone (ITCZ).

Using GATE data, Reed et al. (1977) showed that AEWs typically have wavelengths of 2000–6000 km, periods of 3–5 days, and propagate westward at 7–9 m s^{-1}. Burpee (1974) and Reed et al. (1977) also provided the first direct evidence of AEW structure, including cyclonic features and trough dynamics. These characteristics were later found to vary depending on detection and tracking methods (see section 3).

These findings spurred the development of AEW detection techniques, beginning with wave spectral analyses (e.g.,

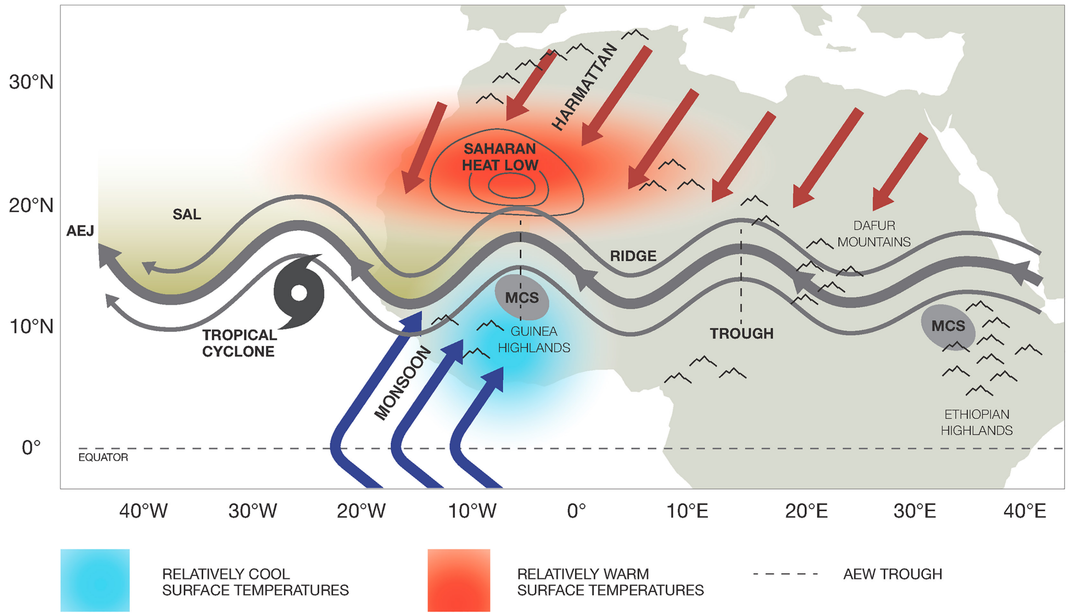

FIG. 1. Adapted from Schwendike (2010), this figure illustrates the horizontal distribution of weather systems over northern Africa and the eastern ATL during the boreal summer.

Norquist et al. 1977; Reed et al. 1988b; Diedhiou et al. 1999; Hsieh and Cook 2005; Kiladis et al. 2006) and later evolving into objective tracking approaches that enabled detailed climatological and statistical studies (e.g., TH01; Berry et al. 2007; Bain et al. 2014; Belanger et al. 2016; Brammer and Thorncroft 2015; Lawton et al. 2022; Hollis et al. 2024).

During GATE, it was also documented that two distinct AEW canonical tracks exist on either side of the AEJ, aligning well with the mixed baroclinic–barotropic instability concept. Observations collected during GATE made it clear, however, that moisture and convection played a larger role in the evolution of these disturbances than previously accounted for and required further investigation (Norquist et al. 1977).

These two AEW tracks are now commonly referred to as the northern track and southern track (Fig. 2). Northern-track waves tend to be drier, characterized by shallow convection with maximum amplitude near the surface (around 850 and 950 hPa). These dry, shallow, low-level waves follow the positive meridional PV gradients over northern Africa (Burpee 1974; Carlson 1969a; Burpee 1972; Reed et al. 1977). In contrast, the southern-track waves are more moist and convectively active with maximum amplitude at the jet level, interacting more strongly with the WAM, making them more favorable for tropical cyclogenesis (Reed et al. 1977; Landsea 1993; TH01; Avila et al. 2000; Russell et al. 2017; Núñez Ocasio et al. 2021). Waves traveling along these two pathways may eventually merge over the Atlantic Ocean, with some studies suggesting that these merged waves can develop into TCs (e.g., Hankes et al. 2015; Duvel 2021; Jonville et al. 2025).

It is now widely recognized that southern-track AEWs are closely linked to monsoonal and orographic convection. These waves derive energy from instabilities within the AEJ, as well as from vertical shear that arises between the monsoon flow and the AEJ itself (e.g., Hsieh and Cook 2005; Nicholson 2009; TH01; Pytharoulis and Thorncroft 1999; Hamilton et al. 2017, 2020; Núñez Ocasio et al. 2021; Emanuel 2026). Indeed, much of the current understanding of Atlantic tropical cyclogenesis—and the mechanisms proposed to explain how AEWs become favorable “seeds” for TCs—has focused on southern-track waves.

The subsequent development of an AEW into a TC also depends on broader large-scale environmental and climatological conditions (e.g., Gray 1968; Bercos-Hickey et al. 2017, 2020; Bercos-Hickey and Patricola 2025). However, even when an AEW is well-structured and environmental conditions appear favorable, a TC does not always form from it in the Atlantic. This is because AEW-driven tropical cyclogenesis (especially southern-track AEWs) also relies on complex convection- and moisture-dependent processes that are difficult to observe and model due to their multiscale nature and spatial variability.

For example, southern-track AEWs are generally more likely to develop into tropical cyclones when they are vertically aligned, convectively in phase (e.g., Hopsch et al. 2010; Leppert et al. 2013; Núñez Ocasio et al. 2020b), moisture enhanced, and favorably embedded within regions of high moisture and convergence in both the immediate and large-scale environments (Hopsch et al. 2010; TH01; Wang 2012; Brammer and Thorncroft 2015; Nam et al. 2023; Núñez Ocasio and Rios-Berrios 2023; Schwendike and Jones 2010). TC genesis may also be aided by a wave-relative critical layer that supports closed circulation, sustained moistening, convection, and vorticity aggregation (e.g., Wang et al. 2010; Asaadi et al. 2017). These characteristics—among other proposed mechanisms—can support the wave’s transition into a TC (Rajasree et al. 2023).

With the continuous high-resolution observation and reanalysis of AEWs, the role of moist convection in initiating, growing, and propagating AEWs has become evident (Fink and Reiner 2003;

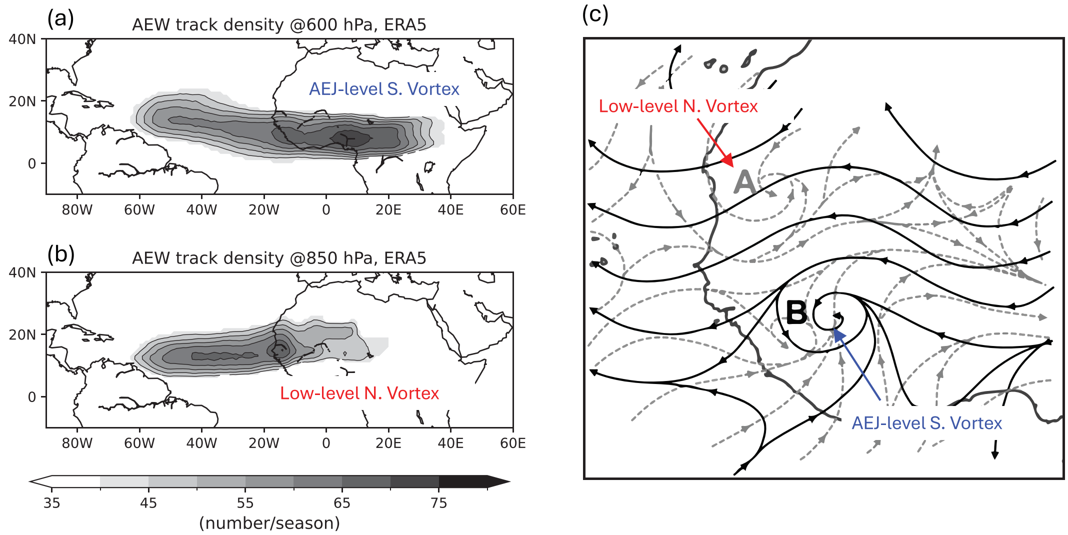

FIG. 2. Track density of AEWs identified from ERA5 (Hersbach et al. 2020) cyclonic vorticity at (a) 600 and (b) 850 hPa from May to October, averaged over 1979–2022, using the tracking method adapted from TH01. (c) Schematic flow patterns for the northern track (low-level northern vortex) and southern track (AEJ-level southern vortex) from Carlson (1969a). In (a) and (b), track density is calculated at each grid point as the number of 6-hourly track points over a 10° × 10° area centered at that point, and for illustration, only values exceeding 40 times per year are shown.

Schwendike and Jones 2010; Mekonnen et al. 2006; Hopsch et al. 2010; Leppert et al. 2013; Zawislak and Zipser 2014; Janiga and Thorncroft 2016; Tomassini et al. 2017; Núñez Ocasio et al. 2020d,b; Núñez Ocasio and Moon 2024; Mayta et al. 2025b; Martinez et al. 2025). As such, the linear normal-mode instability of the AEJ (Burpee 1972) has shown limitations in fully explaining the initiation and growth of AEWs. While there is a spectrum of perspectives, two primary views have emerged regarding AEW initiation and growth: the traditional dynamical view, which attributes their formation strictly to the instabilities in the AEJ, and a relatively recent view, which emphasizes the additional contribution of upscale forcing and diabatic heating due to convection.

In the early 2000s, cases of AEWs that developed into TCs in the Atlantic were first documented as originating from MCSs triggered by the topography of eastern Africa (e.g., TC Alberto 2000; Hill and Lin 2003). Today, the role of convection and upstream topography in the initiation of AEWs is well documented (e.g., Berry and Thorncroft 2005; Thorncroft et al. 2008; Mekonnen et al. 2006; Hill and Lin 2003; Schwendike and Jones 2010; Carlson 1969b; Hamilton et al. 2020; Núñez Ocasio et al. 2021). For example, Hurricane Helene (2006) originated from convection triggered over the Ethiopian Highlands (Fig. 1) and is a field-campaign case that continues to be studied to this day, given its remarkable evolution and growth sustained by convection (Schwendike and Jones 2010; Arnault and Roux 2010; Núñez Ocasio and Rios-Berrios 2023; Núñez Ocasio et al. 2024). Furthermore, a 21-yr climatology by Núñez Ocasio et al. (2021) shows that AEWs initiating over eastern Africa and crossing the west coast are more likely to undergo tropical cyclogenesis than those originating in central or western Africa, serving as a potential key TC genesis predictor. They show that AEWs initiating over eastern Africa have a more pronounced low-level structure, are more convectively active from the onset, and are maintained by anomalous low-level convergence compared to those that initiate farther downstream. African topography has also been shown to play a significant role not only in AEW initiation but also in their energetics, through modulation of the meridional temperature gradient (Hamilton et al. 2017, 2020).

While dry Rossby wave dynamics proved relevant for understanding the formation stages of AEWs, once fully developed, Berry and Thorncroft (2005), in their analysis of TC Alberto's origin over Darfur, and later Thorncroft et al. (2008), proposed that PV anomalies generated by diabatic heating from deep convection could contribute to the initiation, maintenance, and westward propagation of AEWs. They suggested that the framework of diabatic Rossby waves (Parker and Thorpe 1995) offers a bridge between the two leading theories of AEW initiation: one attributing AEW formation to PV anomalies generated by convection and the other to AEWs evolving along preexisting PV gradient associated with AEJ instability. This connection is supported by the observation that convectively generated PV anomalies often reside within the background PV maximum, allowing both mechanisms to interact. This unified perspective allows AEWs to be more consistently interpreted as convectively coupled Rossby-like waves.

This hypothesis has spurred the use and development of a variety of conceptual models such as stratiform instability (or variations of it) (Kuang 2008; Mapes 2000; Russell et al. 2020; Russell and Aiyyer 2020), the weak temperature gradient approximation (Sobel et al. 2001; Hannah and Aiyyer 2017), and moisture mode theory (Núñez Ocasio and Rios-Berrios 2023; Martes et al. 2023) although there is still some debate among them. For example, while Russell and Aiyyer (2020) argue for a more stratiform, vertically upright instability for

AEW growth and maintenance—more dependent on upscale forcing than the diabatic Rossby wave model—Núñez Ocasio et al. (2024) show AEW vertical structures more consistent with barotropic–baroclinic growth. Similarly, while Martes et al. (2023) argue that AEWs in Africa do not satisfy the conditions to be moisture modes, Núñez Ocasio and Rios-Berrios (2023) propose a hybrid evolution in which the disturbances become more moisture mode like as they increasingly interact with the monsoon. Another hybrid hypothesis, proposed by Cheng et al. (2019), suggests that in some instances, AEWs can be considered hybrid combinations of typical AEW and mixed Rossby–gravity (MRG) wave structures, with vertical structures consistent with initial dry Rossby wave dynamics. These models, together with traditional energy and vorticity budgets, support the application of different forms of PV budgets that explicitly account for diabatic moist convection processes, distinct from purely adiabatic processes.

To this day, however, there remains limited consensus on how moist convection contributes to the complex multiscale nature of AEW initiation, growth, and maintenance, though attempts have been made. For example, Hsieh and Cook (2008) proposed that moist convection contributes to enhanced large-scale baroclinic structures, facilitating growth through more effective dynamic processes. More recently, Núñez Ocasio et al. (2024) suggested that both theories may, in fact, coexist: Deep convection at the wave center helps the wave grow, while temperature anomalies, shaped by the northward temperature gradient over Africa, still play a major role in AEW amplitude and energetics.

The next section overviews the dynamical and thermodynamical structures of AEWs, highlighting how features such as their convective envelope relate to wave growth and, in some cases, subsequent TC genesis.

3. Structure and properties of AEWs

a. AEW wavelength, period, and speed

We first review the fundamental wavelength, period, and speed of AEWs. Many of the historical attempts to quantify these properties have been based on spectral filtering methods, which are used to identify and isolate AEW-related signals in time and/or space; this method is described in more detail in section 4a. Burpee (1972) used cross-spectra filtering to identify a spectral peak of 3–5 days that maximized at 700 hPa and expanded in vertical depth as waves propagated to the west. Burpee (1974) built on this study by including additional stations, atmospheric variables, and surface data, estimating an average AEW zonal wavelength of around 3800 km and a periodicity of 4.5 days. Not long after, Reed et al. (1977) applied a combination of spectral filtering and compositing to widespread observations taken during the GATE campaign, culminating into the most comprehensive understanding of AEW horizontal and vertical structures at the time. This study also revised estimates of AEW propagation and spatial characteristics, estimating an average AEW wavelength of 2500 km that decreased as waves moved westward, a period of 3.5 days, and a westward speed of approximately 8 m s^{-1}.

Estimates of the typical frequency and wavenumber characteristics of AEWs, however, have evolved over time. For example, compared to earlier studies, Kiladis et al. (2006) estimated much larger AEW wavelengths of near 4000 km, a 4-day periodicity, and phase speeds that ranged from 8.5 to 12.5 m s^{-1}. The recent spectral power diagrams (see section 4a) computed by Russell and Aiyyer (2020) more closely resemble the results of Kiladis et al. (2006) than the early GATE analyses, with spectral power concentrated at longer wavelengths and periodicities consistent with the Kiladis et al. (2006) findings (Fig. 3). Furthermore, studies have noted differences in AEW phase speed and wavelength as a function of longitude, both decreasing as waves propagate westward (Reed et al. 1977; Diedhiou et al. 1999; Kiladis et al. 2006). This likely relates to changes in the background state as a function of longitude (Kiladis et al. 2006). However, while AEWs are largely advected by the background zonal wind (e.g., Berry and Thorncroft 2005; Russell and Aiyyer 2020), some studies suggest that the embedded moisture and associated convection can slow propagation through interactions with the mean flow (Kiladis et al. 2006; Cornforth and Hoskins 2009; Tomassini et al. 2017; Russell and Aiyyer 2020; Núñez Ocasio et al. 2024).

While many of these previous findings have relied on spectral filtering, similar results have been found using manual and objective tracking techniques. Fink and Reiner (2003) manually identified AEW objects using meridional wind and found wavelengths that ranged from 2200 to 3000 km. Similarly, Bain et al. (2014) used automated tracking of curvature vorticity to estimate typical AEW wavelengths ranging from 2700 to 3700 km. Numerous other wave identification techniques have found AEW phase speeds ranging from 5 to 12 m s^{-1}, with speeds primarily concentrated in the 8–10 m s^{-1} range (Fink and Reiner 2003; Berry et al. 2007; Bain et al. 2014; Lawton et al. 2022).

Differences in estimated wavelength and periodicity across studies likely stem in part from variations in wave identification methods and, in particular, study location. Of note is that our discussion so far has primarily focused on AEWs that grow along the southern flank of the AEJ. While both southern-track and northern-track AEWs grow through mixed barotropic and baroclinic energy conversions, their dominant mechanisms differ. Southern-track AEWs are driven primarily by barotropic energy conversion from the AEJ's horizontal wind shear at the jet level, with latent heat release from deep moist convection providing substantial amplification. Northern-track AEWs were initially characterized as strongly baroclinic, driven by thermal gradients associated with the Saharan heat low (Burpee 1974; Reed et al. 1988a; Pytharoulis and Thorncroft 1999; Chen 2006; Jonville et al. 2025). Recent studies, however, have revealed that northern-track AEWs exhibit predominantly barotropic horizontal structure during their mature phase, despite initiating within a baroclinic environment (Russell and Aiyyer 2020; Mayta et al. 2025a), suggesting stage-dependent energy conversion pathways.

Relatedly, the northern-track waves have been shown to differ in their structure and propagation characteristics from the southern AEWs. For example, Diedhiou et al. (1999) found that AEWs north of the jet exhibited shorter wavelengths and slower phase speeds (3000 km and 8 m s^{-1}) than waves south of the jet (5000 km and 12 m s^{-1}). More recently, work by Jonville et al. (2024, 2025) showed that filtering using different time period windows could distinguish the two types

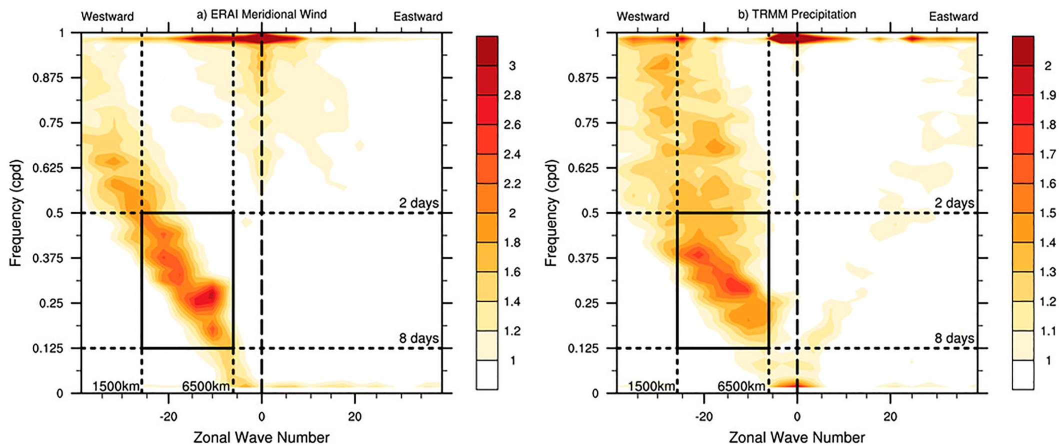

FIG. 3. From Russell and Aiyyer (2020), showing the wavenumber–frequency power spectrum of (a) 650-hPa meridional wind and (b) precipitation taken from July to September 1998–2010 and between 60°E–60°W and 5°–15°N. Values are the ratio of raw spectrum against smooth red noise background, with their chosen "AEW" scale represented by the solid box. Wind data were obtained from the ERA5-Interim reanalysis dataset, and precipitation data are from the Tropical Rainfall Measuring Mission (TRMM). American Meteorological Society. Used with permission.

of wave tracks: 2.95–4.55 days for the southern track and 4.55–6.35 days for the northern track. Using these definitions, they found that the southern track had mean speeds of 8.2 m s^{-1}, whereas the northern track had a slower mean phase speed of 5.8 m s^{-1}. These findings highlight the persistent differences in AEW dynamics and properties between the two wave tracks.

b. *Horizontal structure*

We now turn from wave kinematics to wave structure and dynamics. Early investigations into the horizontal structure of AEWs laid the foundation for understanding their role in tropical meteorology and Atlantic tropical cyclogenesis. Reed et al. (1977) leveraged detailed observations from the GATE field campaign to provide high-resolution descriptions of AEW morphology, including their spatial structure and vertical development. Together, these studies offered the first robust observational basis for the horizontal and vertical characteristics of AEWs, forming the cornerstone of modern AEW theory.

Figure 4, adapted from Reed et al. (1977), provides a composite analysis of the horizontal wind circulation associated with AEWs at multiple vertical levels, using data from the GATE field campaign. The strongest and most coherent cyclonic structure appears at 850 hPa, centered just southwest of the AEW's characteristic inverted trough (relative to midlatitude), which is evident at the 700-hPa stagnation point of the meridional wind. This suggests that 700 hPa is the level of maximum AEW amplitude, as measured by the circulation. The region of the inverted trough with positive meridional winds is called the southerlies, while the region with negative meridional winds is called the northerlies. At the surface, convergence into the wave trough is evident, while the structure at 200 hPa becomes more zonal. The progressive eastward tilt below 700 hPa indicates baroclinic energy conversion from low-level temperature gradients, while the westward tilt above 700 hPa reflects barotropic energy extraction from the AEJ, confirming the mixed barotropic–baroclinic structure characteristic of southern-track AEWs, with baroclinic processes being particularly pronounced at lower levels. Between 700 and 650 hPa, the core of the AEJ lies between 12° and 15°N, where notable meridional wind shear is present, and PV anomalies associated with southern-track AEWs are tilted upshear in the horizontal plane and centered near the jet axis (Fig. 5), aligning with regions of weak or negative background meridional PV gradient (Raj et al. 2023; Russell and Aiyyer 2020). In contrast, the circulation maximum of northern-track AEWs is primarily found at 925 hPa near 20°N, where the background flow shows minimal meridional shear and the wave tilt is less pronounced, indicating a barotropically unstable environment, particularly in the midtroposphere following recent findings (Janiga and Thorncroft 2013; Russell and Aiyyer 2020; Mayta et al. 2025a).

Following the foundational work of Reed et al. (1977) and the GATE campaign, the era of satellite observations, and a new wave of field programs—including NASA's African monsoon multidisciplinary analyses (NAMMA) and African monsoon multidisciplinary analyses (AMMA) in 2006 (Zipser et al. 2009; Redelsperger et al. 2006)—provided significantly improved representations of the horizontal structure of AEWs. The NAMMA campaign focused on the development of AEWs and their relationship to tropical cyclogenesis off the West African coast, utilizing aircraft and satellite observations to reveal how MCSs interact with AEW troughs, particularly highlighting the importance of moisture transport, SAL interactions, and low-level convergence zones. In parallel, AMMA offered a more comprehensive, continental-scale view of AEWs and the WAM system, providing insights into wave initiation over the Ethiopian Highlands, wave-mean flow interactions, and the role of convective organization in modulating AEW structure and strength.

The 2006 AEW cases of Tropical Storm Debby and Hurricane Helene remain key case studies due to their observational

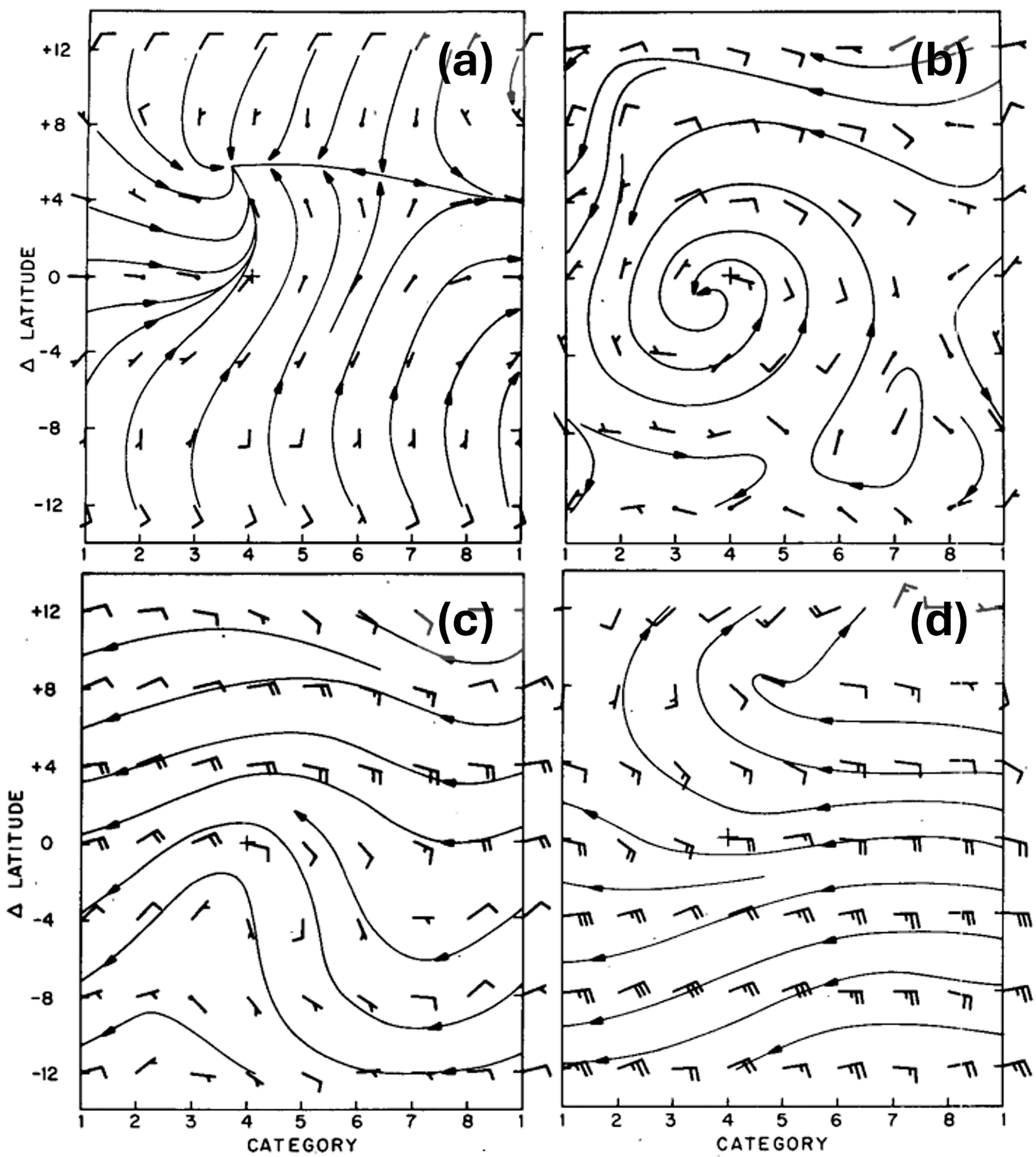

FIG. 4. Adapted from Reed et al. (1977), this figure depicts streamlines and wind barbs [from GATE observations showing the horizontal wind and circulation structure of AEWs at four pressure levels: (a) surface, (b) 850 hPa, (c) 700 hPa, and (d) 200 hPa]. The *x* axis represents wave phase "category," from 1 to 8, while the *y* axis shows latitude relative to the AEW trough.

coverage during NAMMA and their illustration of AEW–MCS coupling in tropical cyclogenesis (e.g., Berry and Thorncroft 2005; Lin et al. 2013; Sippel et al. 2011; Schwendike and Jones 2010; Arnault and Roux 2010; Núñez Ocasio and Rios-Berrios 2023; Núñez Ocasio et al. 2024; Núñez Ocasio and Dougherty 2024). Though it was not until the climatological work by Núñez Ocasio et al. (2021) that eastern-origin AEWs were statistically linked to higher genesis potential, the pre-Debby and pre-Helene were among the first such observed AEWs, underscoring the role of topography in AEW–MCS interactions. In Helene's case, strong convection developed ahead of the wave trough over coastal and oceanic regions—where convective available potential energy (CAPE) and low-level convergence peaked—while sustained MCS activity over land coincided with the 700-hPa trough. High-resolution kilometer-scale modeling has since revealed moisture–convection feedbacks and identified the pre-Helene wave as a possible moisture mode due to strong moisture gradients (Núñez Ocasio et al. 2024).

More recently, the 2022 Convective Processes Experiment–Cabo Verde (CPEX-CV) campaign (Nowottnick et al. 2024; Martinez et al. 2025) obtained state-of-the-science observations of AEWs through the use of cutting-edge airborne

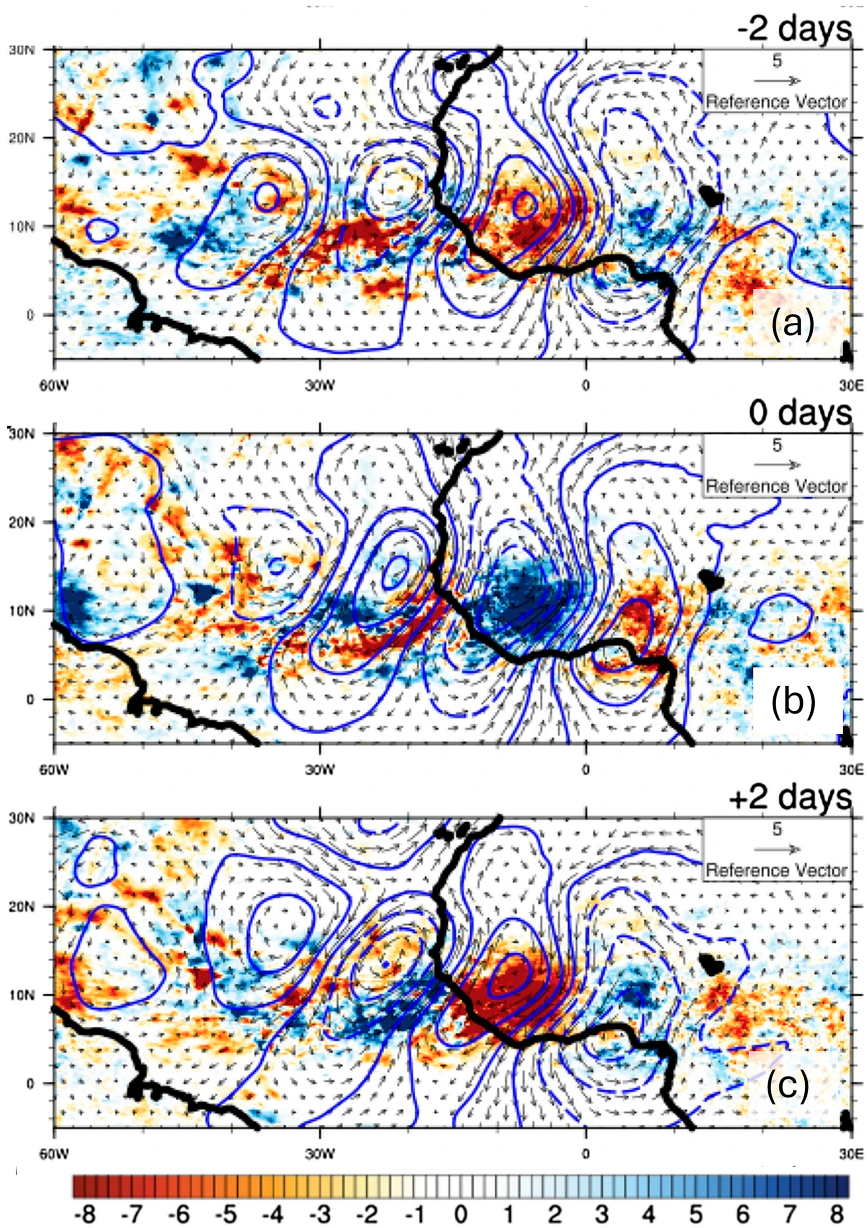

FIG. 5. Figure adapted from Raj et al. (2023), (a)–(c) Composite anomalies for 3–5-day AEWs from −2 to +2 days for the IMERG precipitation dataset (Huffman et al. 2019) precipitation and ERA5 wind field data from 1979 to 2004. Vectors are 700-hPa wind anomalies (m s^{-1}). Blue contours are the streamfunction. Rainfall anomalies (mm day^{-1}) are shaded.

instrumentation (e.g., from dual- to triple-frequency radar and Doppler wind lidar aboard research aircraft), integrated with high-resolution satellite products such as Integrated Multisatellite Retrievals for GPM (IMERG), and modern reanalysis data like fifth generation ECMWF atmospheric reanalysis (ERA5). These resources, which were not available during or prior to 2006, enabled CPEX-CV to provide a more comprehensive view of AEWs—capturing a more up-to-date view of their life cycle from West Africa into the Atlantic. The campaign obtained views of the three-dimensional structure of AEWs interacting with convection, dry-air intrusions, moist inflows, and the marine boundary layer. These recent efforts highlight the complex, multiscale dynamics of AEWs and their central role in tropical weather and climate variability.

A stark comparison between the NAMMA and CPEX-CV field campaigns, in terms of data resolution and availability, is shown in Figs. 6a and 6b. The 2022 datasets provide much higher temporal and spatial resolution, enabling improved analysis of short-term AEW–MCS variability. This figure includes the use of objective tracking techniques to monitor

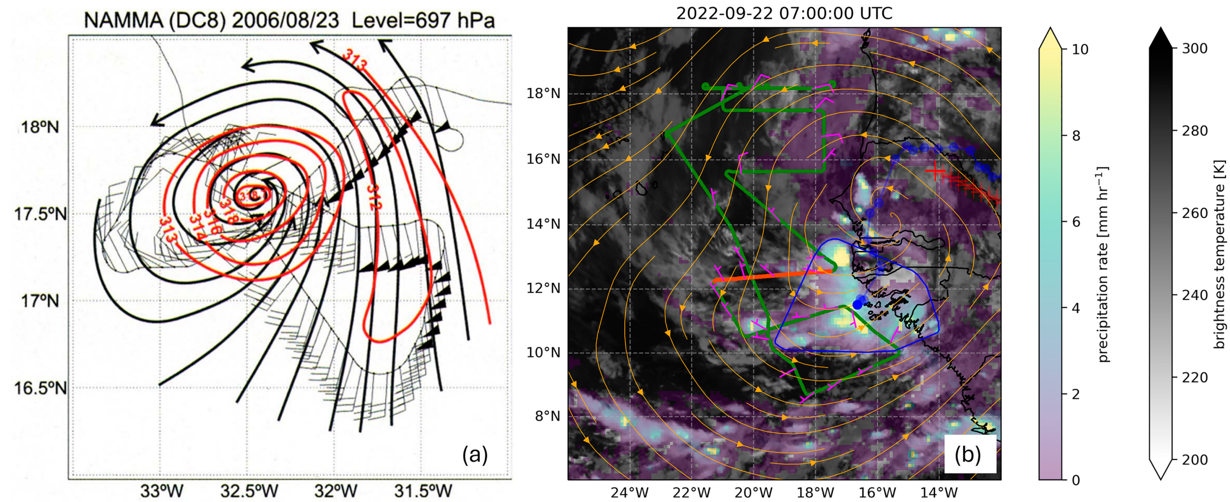

FIG. 6. The combined images illustrate the evolution of field campaign analysis. Adapted from Zipser et al. (2009), (a) a NAMMA DC-8 flight near the Tropical Storm Debby (2006) center on 23 Aug 2006, collecting remote sensing and dropsonde data. Debby's inner structure is presented, with red lines for potential temperature, thick gray lines as streamlines, a thin gray line for the flight path, and wind barbs representing 10 and 50 kt (1 kt ≈ 0.51 m s^{-1}). (b) The track of CPEX-CV Research Flight 9 (green) at 0700 UTC 22 Sep 2022, with 850-hPa ERA5 streamlines (orange), 1000-hPa dropsonde wind barbs (magenta), IMERG rainfall (winter shading), Meteosat brightness temperature (gray shading), and track of MCSs [blue, via Tracking Algorithm for Mesoscale Convective Systems (TAMS); Núñez Ocasio et al. 2020d; Núñez Ocasio and Moon 2024] and AEW (red, via Lawton et al. 2022).

both MCS and AEW evolution. The highlighted case in Fig. 6b is of an AEW observed during the morning hours of 22 September 2022, which later developed into Hurricane Hermine (2022). In this case, convection and rainfall were concentrated southwest of the 850-hPa wave-centered trough, with convection largely influenced by coastal atmospheric processes.

Prior to 2022, Janiga and Thorncroft (2016) provided a more complete view of the climatological AEW–convection/MCS relationship (Figs. 7a,b) using reanalysis products and satellite-derived products. They showed that AEWs modulate convection differently over central West Africa (CWA) and the Atlantic (ATL). Over CWA, the northerlies phase features enhanced low-level moisture, warmer temperatures, and high CAPE, driving strong ascent and peak rainfall. This is consistent with Schlueter et al.'s (2019) findings of enhanced shear and CAPE ahead of the trough. Convective rainfall occurs ahead of the trough, in the region of the northerlies, while stratiform rainfall is more common in the trough. Over the ATL, rainfall peaks in the trough phase, mainly due to higher column moisture, despite weaker ascent. These differences reflect how local thermodynamic conditions shape AEW–convection interactions. Results from Janiga and Thorncroft (2016) align with NAMMA observations. It is important to note, however, that it is a common behavior of parameterized convection, such as in ERA5, and even in observational products like IMERG, to exhibit rainfall maxima in the trough over land as well (e.g., Fischer et al. 2024).

Earlier, Fink and Reiner (2003) highlighted differences in AEW–MCS interactions between northern- and southern-track waves: In the north, MCSs often form ahead of and behind the trough, whereas in the south, they tend to develop near or ahead of it. Enhanced convection behind northern troughs is linked to moisture transport from the ocean and equatorial forests. The modulation of convection by AEWs has also been shown to be one driver of extreme rainfall events over continental Africa (Nicholls and Mohr 2010; Crétat et al. 2015; Lafore et al. 2017).

It is now well established that the alignment between the AEW trough and MCSs or convection enhances midlevel vorticity, especially for southern-track AEWs, where vortex stretching and PV generation result from diabatic heating (e.g., Schwendike and Jones 2010; Semunegus et al. 2017; Tomassini et al. 2017; Núñez Ocasio et al. 2020b; Russell et al. 2020). As shown in Figs. 7c and 7d, lower–midtropospheric moisture convergence at or just ahead of the trough initiates and organizes convection, with vortex stretching contributing to wave amplification (Tomassini et al. 2017). When convection shifts ahead of the trough and becomes out of phase with it, it can instead accelerate AEW propagation. While AEWs propagate at approximately 8 m^{-1} (Fink and Reiner 2003; Núñez Ocasio et al. 2020b), MCSs propagate faster—typically between 10 and 12 m s^{-1}—unless they are coupled to the AEW near the trough or just slightly ahead of it, in which case they propagate at approximately the AEW phase speed (Fink and Reiner 2003; Núñez Ocasio et al. 2020b). Over the Sahel, MCSs can propagate at speeds of up to about 15 m s^{-1} (Desbois et al. 1988; Laing et al. 2008; Mathon et al. 2002; Fink and Reiner 2003; Núñez Ocasio et al. 2020d).

The spatial and temporal phasing between convection and the AEW trough plays a key role in supporting wave growth and maintenance. In addition to AEW growth, past studies have documented that the likelihood of tropical cyclogenesis increases when AEWs are effectively coupled with convection and MCSs, particularly when these coupled systems are located

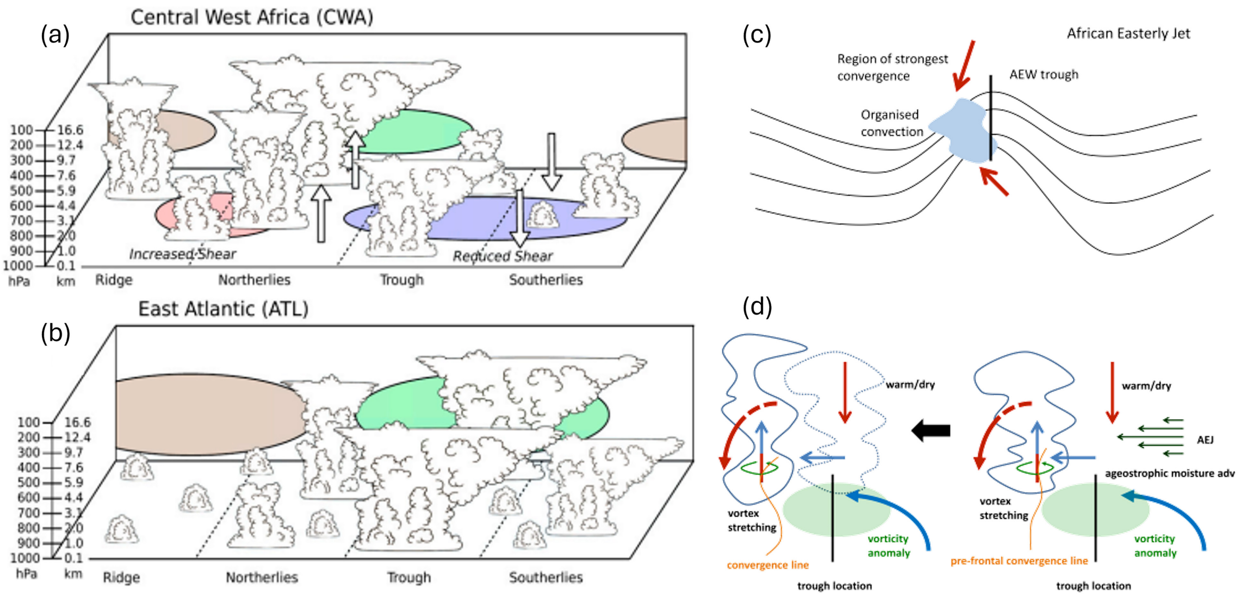

FIG. 7. Adapted from Janiga and Thorncroft (2016), the AEW–convection relationship over (a) CWA and (b) the east ATL, with exaggerated phases to emphasize differences. Green and brown circles indicate regions of positive and negative moisture anomalies, while red and blue circles represent warmer and cooler low-level temperatures, linked to increased or reduced CAPE. Arrows illustrate adiabatic ascent and descent. Based on Tomassini et al. (2017), (c) moisture convergence in the AEJ–AEW system is strongest near and just ahead of the trough, supporting organized convection. (d) A three-dimensional schematic where moist air is advected northward behind the trough and dry air southward ahead, enhancing moisture near the trough. Strong updrafts within MCSs ahead of the trough generate PV through vortex stretching, supporting AEW propagation.

off the western coast of Africa and over the eastern Atlantic (Fink and Reiner 2003; Hopsch et al. 2010; Semunegus et al. 2017; Leppert et al. 2013; Zawislak and Zipser 2014; Wang 2018, 2012; Núñez Ocasio et al. 2020b). The coupling between convection and AEWs is strongly influenced by moisture–convection feedbacks (e.g., Wang 2018; Brammer and Thorncroft 2015; Hopsch et al. 2010; Núñez Ocasio and Rios-Berrios 2023), which are more favorable under active WAM conditions (Hsieh and Cook 2008; Núñez Ocasio et al. 2021). Using a climatology of AEWs that developed into TCs versus those that did not, Núñez Ocasio et al. (2020b) showed that developing AEWs were associated with stronger convection over West Africa and the eastern Atlantic. This convection was more closely aligned with the wave vortex (in both speed and position), exhibited larger cloud shields, and was more intense than in nondeveloping cases. Furthermore, Núñez Ocasio et al. (2020b) documented for the first time that this pattern held not only for waves over West Africa and the eastern Atlantic but also for those still propagating over central Africa. This result highlights the importance of AEW–MCS interactions and their key role in determining the eventual fate of AEW genesis, even prior to reaching the coast.

c. Vertical structure

In addition to their horizontal structure, AEWs also exhibit a unique vertical structure that is inherently tied to their dynamics. As discussed previously, Burpee (1972) provided one of the first depictions of the vertical structure of AEWs through the spectral filtering of upper-air observations. He found that these waves originated near the 700-hPa level, with their depth increasing as they propagated westward. A pronounced vertical tilt, consistent with barotropic–baroclinic energy conversions, provided early observational evidence that background dynamic instabilities supply energy for these waves. A subsequent compositing study of upper-air data (Burpee 1974) confirmed this vertical structure using data from additional observational stations across Africa.

Soon after, detailed surface and upper-air observations from the GATE field campaign were used to build what were then the most comprehensive composites of AEW vertical structure (Reed et al. 1977). Some findings differed from earlier studies. Notably, meridional wind anomalies were shown to be nearly vertical below 700 hPa and then tilted westward above. This discrepancy from Burpee (1972) was partly due to the GATE profiles being taken at more southern latitudes, suggesting that AEWs south of the AEJ derive less energy from baroclinicity and more from latent heat compared to their northern counterparts.

The analysis by Reed et al. (1977) of temperature profiles also showed that AEWs are cold-core systems, with relatively cold air below 700 hPa and warm air above. Meridional and zonal wind fluctuations peaked near 650 hPa, and their covariance indicated a southward transport of easterly momentum. An upper-level (200 hPa) anticyclonic circulation was also observed above AEWs. Additionally, the composite vertical structure further indicated a link between wave dynamics and convection, with low-level convergence and upward motion ahead (west) of the wave trough, coinciding with the observed maximum in brightness temperature. Many of the findings on AEW vertical structure originating from GATE continue to be reaffirmed in studies to this day (e.g., Kiladis et al. 2006; Hopsch et al. 2010; Brammer and Thorncroft 2015; Russell and Aiyyer 2020).

Nevertheless, the advent of modern satellite coverage and reanalysis products has further refined our view of the typical vertical structure of AEWs, their variability, and their connection to the formation of TCs. To study the three-dimensional structure of AEWs and their evolution over a large sample size, Kiladis et al. (2006) projected reanalysis variables onto AEW spectrally filtered brightness temperature (discussed further below). The resulting vertical structure in meridional wind is shown in Fig. 8. Of note are the largely upright lower levels, westward tilt at upper levels, and prominent anticyclone aloft, all of which mirror earlier results from Reed et al. (1977). The position of convection (OLR minimum) changes relative to the meridional wind anomalies over time; it shifts from the northerlies (ahead of the trough) at day −2, then into the trough, and eventually the southerlies at days 0 and +2. The analysis conducted by Kiladis et al. (2006) also allowed for a more comprehensive analysis of the vertical distribution of specific humidity. They noted high levels of specific humidity ahead of the trough axis (in the northerlies) that are subsequently lifted into mid- and upper-tropospheric levels at the wave trough. This, they found, differed from the composites of Reed et al. (1977), likely due to north–south differences in the sample locations used in each study.

AEW vertical structure varies based on a wave's latitudinal position. As discussed earlier, northern-track AEWs (north of the AEJ, roughly 10°N) are often thought to be more baroclinic than those to the south, resulting in notable vertical tilts and wave growth that is more closely tied to thermal instability. Meanwhile, southern-track AEWs (south of the AEJ, roughly 10°N) are more barotropic at the jet level and characterized by weaker temperature gradients and dynamics dominated by vorticity advection and diabatic processes and as a result have a more vertically stacked structure even from the initial stages (e.g., Reed et al. 1977; Burpee 1972; Diedhiou et al. 1999; Kiladis et al. 2006; Hopsch et al. 2007; Cheng et al. 2019). However, as noted in the previous section, recent work has challenged the role of baroclinicity as a substantial driver of easterly waves and their structure, even though their vertical tilt and environment often resemble those of baroclinic waves (as is the case for many northern-track AEWs) (Russell and Aiyyer 2020; Mayta et al. 2025a).

Recent research has focused on the connections between the vertical structure of AEWs and TC genesis. Hopsch et al. (2010) compared vertical composites of AEWs that did and did not result in TC formation in a 40-yr reanalysis dataset. They found that developing waves typically show a strengthening low-level circulation accompanied by a transition from a cold-core structure to a warm-core structure. In contrast, nondeveloping AEWs tend to maintain weaker low-level circulations and remain cold core. Notably, nondeveloping waves—even intense ones—often have dry mid–upper-level air west of the trough. Subsequent studies highlighted the role of lower-tropospheric moisture northwest of the wave trough in increasing the probability of TC formation (Brammer and Thorncroft 2015, 2017). Waves lacking a strong, vertically aligned circulation

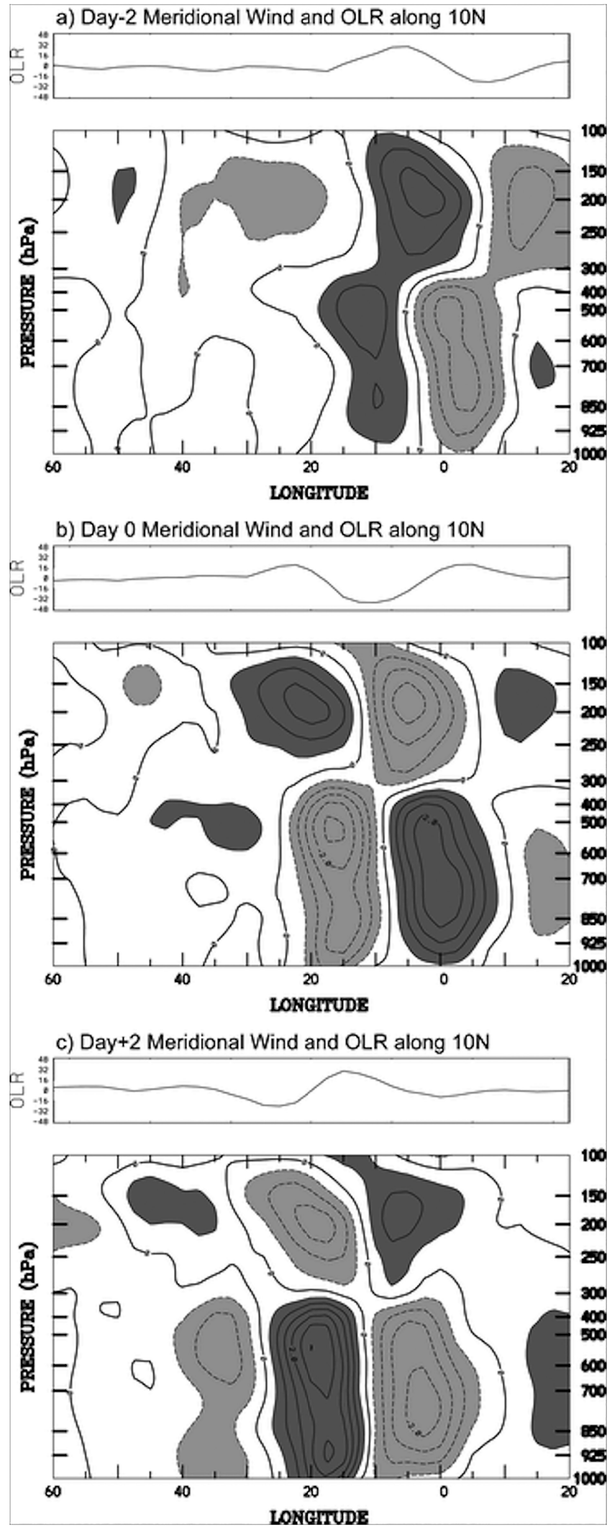

FIG. 8. Adapted from Kiladis et al. (2006) showing zonal–height cross sections of anomalous meridional wind taken along 10°N and regressed against TD-filtered OLR at a base point of 10°N, 10°W. The (a) day −2, (b) day 0, and (c) day +2 lagged regressions. The contour interval is 0.5 m s^{-1}, and negative contours are dashed. The associated OLR anomaly is shown at the top (W m^{-2}).

are more prone to dry-air intrusions that undercut the midlevel vortex, promoting decay, suppressing convection, and ultimately weakening the system (Brammer et al. 2018). Indeed, the presence of a strong low-level circulation has been shown to be statistically important for wave intensification and TC genesis (Brammer and Thorncroft 2015; Lawton and Majumdar 2023), as has the vertical extent of diabatic heating and its relationship to the external environment (Núñez Ocasio et al. 2020b, 2024; Russell et al. 2020).

Several studies have demonstrated that the vertical structure of AEWs is intrinsically connected to moist convection, with substantial evidence that convection plays a major role in AEW growth and propagation (i.e., Kiladis et al. 2006; Hall et al. 2006; Berry and Thorncroft 2012; Núñez Ocasio et al. 2020d,b, 2024; Russell and Aiyyer 2020; Russell et al. 2020). This relationship also illustrates why the shift in deep convection from the northerlies to within the wave trough as AEWs move offshore is important: Over land, diabatic heating associated with deep convection primarily contributes to the propagation of the AEW's low-level circulation, whereas over the ocean it can intensify the lower-level circulation and promote vertical vortex alignment.

It should be noted that this diabatic heating is strongly controlled by the complex interactions between AEWs and MCSs, and as discussed in the previous section, the phasing of MCSs relative to the wave trough has important ramifications for AEW development and associated energy budgets (Alaka and Maloney 2014; Núñez Ocasio et al. 2020d,b, 2024). The shift in peak convection relative to the AEW trough is influenced by the wave's vertical tilt, the environmental vertical shear, and regional moisture availability. Over Africa, convection tends to occur downstream of the trough where low-level convergence is strongest, whereas over the Atlantic, enhanced midlevel moisture and altered shear can allow convection to align more closely with, or even upstream of, the trough (e.g., Berry and Thorncroft 2005; Hopsch et al. 2010; Thorncroft et al. 2008). Over land, convection is also often influenced by the diurnal cycle (e.g., Diedhiou et al. 1999; Hopsch et al. 2010; Wang et al. 2010).

d. *AEW energetics*

To better understand and quantify the growth and propagation of AEWs, many previous studies have examined the energy processes of the AEJ–AEW system (Burpee 1972; Norquist et al. 1977; Reed et al. 1988c; Thorncroft 1995; Hsieh and Cook 2007). The potential and kinetic energy equations were first partitioned into their zonal and eddy forms by Lorenz (1955), where he defined the concept of available potential energy (APE), which is the main driver of midlatitude eddies and the general circulation of the atmosphere. Further progress was made by Oort (1964), who identified energy conversion processes and developed methods for separating the total kinetic and APE into their mean and eddy parts in time and space. Muench (1965) built on the work of Lorenz (1955) and derived a set of energy equations that were then used by Norquist et al. (1977) to investigate the energetics of AEWs.

Norquist et al. (1977) found that the kinetic energy of the AEWs is maintained by baroclinic and barotropic conversions from zonal kinetic energy and eddy APE supplied by the zonal APE. In an analysis of the structure and characteristics of AEWs, Reed et al. (1988c) confirmed that AEWs grow as a result of the joint baroclinic–barotropic instability of the AEJ. They additionally found that the baroclinic energy conversions are located north of the AEJ and below the jet level, whereas the barotropic energy conversions are located near the AEJ and extend throughout a layer of appreciable depth (700–400 hPa). These results have been further confirmed by more recent research using over a decade of reanalysis data (Diedhiou et al. 2002). Studies have shown, however, that the energy conversions do not equally contribute to the growth of the AEWs, with wave growth initially dominated by barotropic energy conversions followed by baroclinic energy conversions (Thorncroft and Hoskins 1994a,b; Thorncroft 1995). Barotropic energy conversions may also play a larger role once an AEW exits the coast of Africa, as was demonstrated in an analysis of the AEW that preceded the formation of Hurricane Helene in 2006 (Arnault and Roux 2009).

Early studies hypothesized that AEWs both grew and formed from the combined baroclinic–barotropic instability of the AEJ (Burpee 1972; Reed et al. 1988c). However, a suite of studies that utilized energetics analyses of the AEJ–AEW system found that the instability of the jet was not a key factor in the initiation of the waves (Hsieh and Cook 2005; Kiladis et al. 2006; Hall et al. 2006; Thorncroft et al. 2008). Indeed, Hall et al. (2006) found that without damping, baroclinic and barotropic energy conversions lead to wave growth, whereas a modest amount of low-level damping stabilized the system, indicating that baroclinic–barotropic instability alone could not explain AEW initiation. An alternative method for AEW initiation was proposed by both Thorncroft et al. (2008) and Hsieh and Cook (2005), where some type of latent or convective heating trigger is needed for the wave to form.

Hsieh and Cook (2007) performed a complete energetics analysis of AEWs using energy equations in a similar form to Norquist et al. (1977) but with additional derivations included for completeness that include diabatic generation, dissipation, and boundary flux terms for an analysis in a limited region. The energy equations presented in Hsieh and Cook (2007) have been used by numerous contemporary studies that aim to diagnose the energy processes of AEWs (Grogan et al. 2016; Bercos-Hickey et al. 2017; Russell et al. 2017; Bercos-Hickey and Patricola 2021; Núñez Ocasio et al. 2024; Núñez Ocasio and Dougherty 2024). Using a single season of regional model simulations, Hsieh and Cook (2007) found that baroclinic conversions are the dominant energy source of the AEWs, although barotropic conversions can make significant contributions when there is convective activity south of the AEJ. In a study of the intraseasonality of AEWs, Alaka and Maloney (2014) also found barotropic energy conversions dominate south of the AEJ, although the combined baroclinic–barotropic energy conversions were important for maintaining intraseasonal AEW activity in West Africa. These results highlight the importance of different spatial scales, where the large-scale flow and convective scales are both important for the

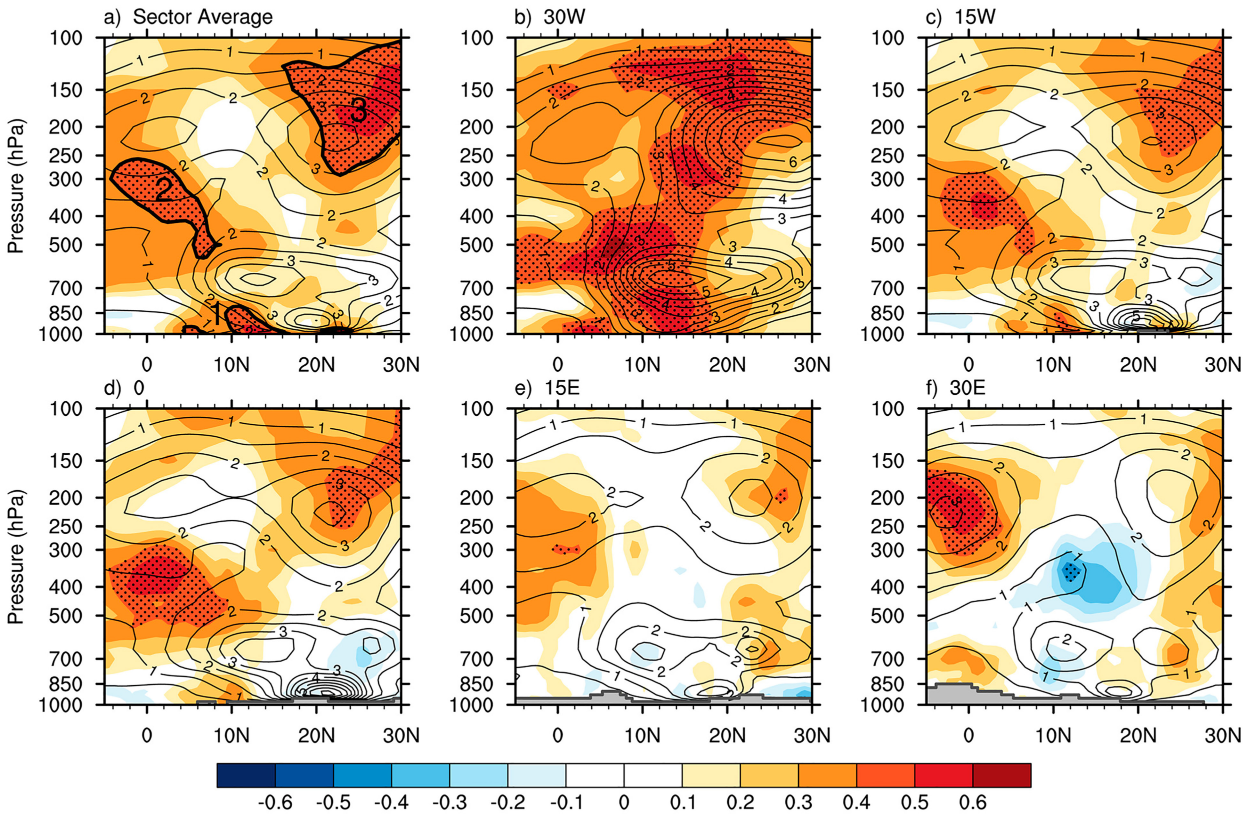

FIG. 9. From Russell et al. (2017) showing latitude–height cross sections of the correlation between the number of TCs with AEW origins and seasonal-mean EKE (filled) for (a) 30°W–30°E, (b) 30°W, (c) 15°W, (d) 0°, (e) 15°E, and (f) 30°E. Contours represent the seasonal-mean EKE (J kg^{-1}), and stippling represents statistical significance of 95% for the correlations. Outlined areas with numbers represent specific statistically significant areas of correlation discussed in Russell et al. (2017).

growth of AEWs. Indeed, convective activity has been shown to contribute to the growth of AEWs north and south of the AEJ through the conversion of eddy APE to eddy kinetic energy (EKE). South of the AEJ, moist convection associated with the West African monsoon contributes to the diabatic generation of eddy APE (Hsieh and Cook 2007; Bercos-Hickey et al. 2022), whereas north of the AEJ dry convection contributes to both the diabatic generation of APE and the conversion of zonal APE to eddy APE through the enhancement of the meridional temperature gradient (Lau and Lau 1992).

Energetics analyses of AEWs have recently been used in studies that have focused on the relationship between AEWs and tropical cyclogenesis, the effects of Saharan dust on AEWs, and the impact of climate change on AEWs. Using EKE as a proxy for AEW activity, Russell et al. (2017) found that a correlation between seasonal-mean EKE and tropical cyclogenesis was maximized in the lower troposphere below the southern AEW track (Fig. 9). Additionally, an energetics analysis of high-resolution global model data was used to show that AEWs that develop into tropical cyclones have larger EKE than the nondeveloping waves (Bercos-Hickey et al. 2023). Idealized and realistic regional modeling studies have also shown that the radiative effects of Saharan dust aerosols strengthen the EKE of AEWs through diabatic heating, preferentially in the north wave track (Grogan et al. 2016; Bercos-Hickey et al. 2017). With respect to climate change, studies have found a robust future increase in AEW strength and frequency that was attributed to increases in the baroclinic and barotropic energy conversions and an associated strengthening of the meridional temperature gradient over West Africa (Bercos-Hickey and Patricola 2021; Akinsanola et al. 2025).

4. AEW tracking

Due to the multiscale nature of AEWs, the identification of individual wave phases has remained a nontrivial task. An individual AEW trough can include multiple MCSs propagating faster than the wave, and multiple vortices at different isobaric levels and different spatial and temporal scales; therefore, tracking the AEW itself includes levels of subjectivity on the scale of the disturbance of particular interest. The focus of the majority of research on AEWs has identified the trough of the wave as the feature of interest and in particular that has been almost exclusively the focus of AEW tracking papers.

a. *Spectral filtering*

One of the earliest tools used to identify AEWs was spectral filtering, dating to the early 1960s (e.g., Rosenthal 1960).

Because the tropical atmosphere contains variability across many scales, spectral filtering helps isolate the dominant periodicities (and wavelengths) associated with coherent wave phenomena. Many have pointed to the work by Yanai et al. (1968) as a turning point for the application of spectral filtering to the tropics (Maloney and Zhang 2016; Takayabu et al. 2016). In their seminal study, Yanai et al. (1968) computed time power spectra for several west Pacific radiosonde stations and identified propagating wave features with distinct characteristics. These included coherent features with a 3–5-day periodicity, which appeared similar to easterly waves identified in prior studies. This spectral filtering technique was soon shown to be effective at identifying various tropical phenomena, such as equatorial waves, the Madden–Julian oscillation, and AEWs (Wallace and Chang 1969; Yanai and Murakami 1970; Madden and Julian 1971; Burpee 1972).

Modern research has leveraged the known spectral characteristics of AEWs to isolate them from other propagating features in the tropics (Hayashi 1982; Wheeler and Kiladis 1999; Kiladis et al. 2009). Most filtering techniques fall into two categories: 1) exclusively filtering signals in time or 2) filtering signals in both space and time. For time-based filtering, environmental fields are often bandpass filtered using a periodicity range of 2–6 days—though some studies have used upward of 10 days—such that only signals within this range are retained (e.g., Mekonnen et al. 2006; Jiang et al. 2023). For space and time filtering, environmental fields are generally filtered using both periodicity and zonal wavenumber (e.g., Kiladis et al. 2006; Russell and Aiyyer 2020).

An example from Russell and Aiyyer (2020) of the spectral power for meridional wind and precipitation was shown previously in Fig. 3. They chose a spectral filtering window based on the region with the highest magnitude powers, in this case between wavenumbers −6 and −26 and periods of 2 and 8 days. Others have further bounded this spatiotemporal filtering with equivalent depth curves, in an attempt to more directly capture the observed spectral peaks associated with easterly waves (Kiladis et al. 2006; see their Fig. 1). This region in frequency–wavenumber space is often referred to as the "tropical depression (TD) band."

b. *Hovmöller plot analysis and manual tracking*

Spectral filtering methods originally identified AEWs as westward-propagating features. However, there was a need to follow the evolution of these waves through time. Through a combination of satellite imagery and streamline analysis of radiosonde data, it was found that disturbances could be identified and manually tracked across western Africa and the eastern Atlantic (Carlson 1969b; Burpee 1974). Subsequent studies identified 850 and 700 hPa as key levels for tracking AEW troughs, with spectral filtering and Hovmöller diagrams (longitude–time diagrams; see Fig. 11a for an example) assisting in identifying consistent westward-propagating signals (Hovmöller 1949; Nitta and Takayabu 1985; Reed et al. 1988b).

Hovmöller plots provide additional spatial smoothing by averaging the chosen field over a latitudinal band, enabling features to be tracked across longitudes and through time with relative ease. These plots were used to identify the transition of meridional wind from northerly to southerly, thereby locating the trough of the wave. Spectral or bandpass filters have also been leveraged to emphasize the westward-propagating signal of AEWs and to identify multiple latitudes of AEW activity, with peaks occurring at 7.5° and 20°N (Duvel 1990) or 5° and 15°N (Diedhiou et al. 1999). Hovmöller plots not only enable the visual identification of AEW troughs but also allow the tracking of westward-propagating disturbances within the chosen latitude band. Pytharoulis and Thorncroft (1999), for example, used a combination of isobaric levels and latitudinal bands to track AEWs north and south of the AEJ and found that the two disturbances were typically coherent features that propagated together.

While averaging over latitude bands to construct a Hovmöller plot emphasizes the trough of a typical meridionally oriented AEW, the method lacks the latitudinal position of the circulation center and struggles to identify weak or zonally tilted troughs. Therefore, Fink and Reiner (2003) developed a multistep tracking methodology to refine the positional location of the trough circulation. The first step of their method still utilized Hovmöller plots generated at 700 hPa (7°–13°N) and 850 hPa (17°–23°N) to identify the longitude of the AEW trough axis. Bandpass-filtered winds at 850 hPa were then used to identify low-level circulation centers, with 700 hPa used as a fallback if the low-level circulation was ambiguous. Although still manual, this methodology highlighted the benefits of combining Hovmöller plot analysis with isobaric analysis to refine AEW features.

This manual multistep method was also used by Chen (2006) to backtrack northern and southern disturbances from AEW troughs identified at the coast of West Africa over a 10-yr period and extended to a full 40-yr record by Chen et al. (2008), but limited to tropical disturbances identified by the National Hurricane Center (NHC) over the Atlantic. Kerns et al. (2008) extended this multistep tracking to include all easterly waves across the Atlantic for a shorter 4-yr period.

Berry et al. (2007) introduced objectively defined trough axis lines, based on the advection of curvature vorticity, and used these trough lines to manually track waves through time, refining latitudinal position based on the intersection of the trough axis with the AEJ. The use of curvature vorticity better distinguishes the wave trough from vorticity contributed by the background horizontal shear.

Although these manual methods produced high-quality curated tracks of AEWs, the studies were typically limited in scope due to the resources required for manual tracking, often restricting analysis to individual seasons.

c. *Objective and feature-based tracking*

As manually tracking AEWs became too labor intensive for large datasets, the need for automated, objective tracking techniques increased. The developments in manual tracking strongly influenced the design of automated approaches, the history of which can be traced in an AEW tracker family tree (Fig. 10).

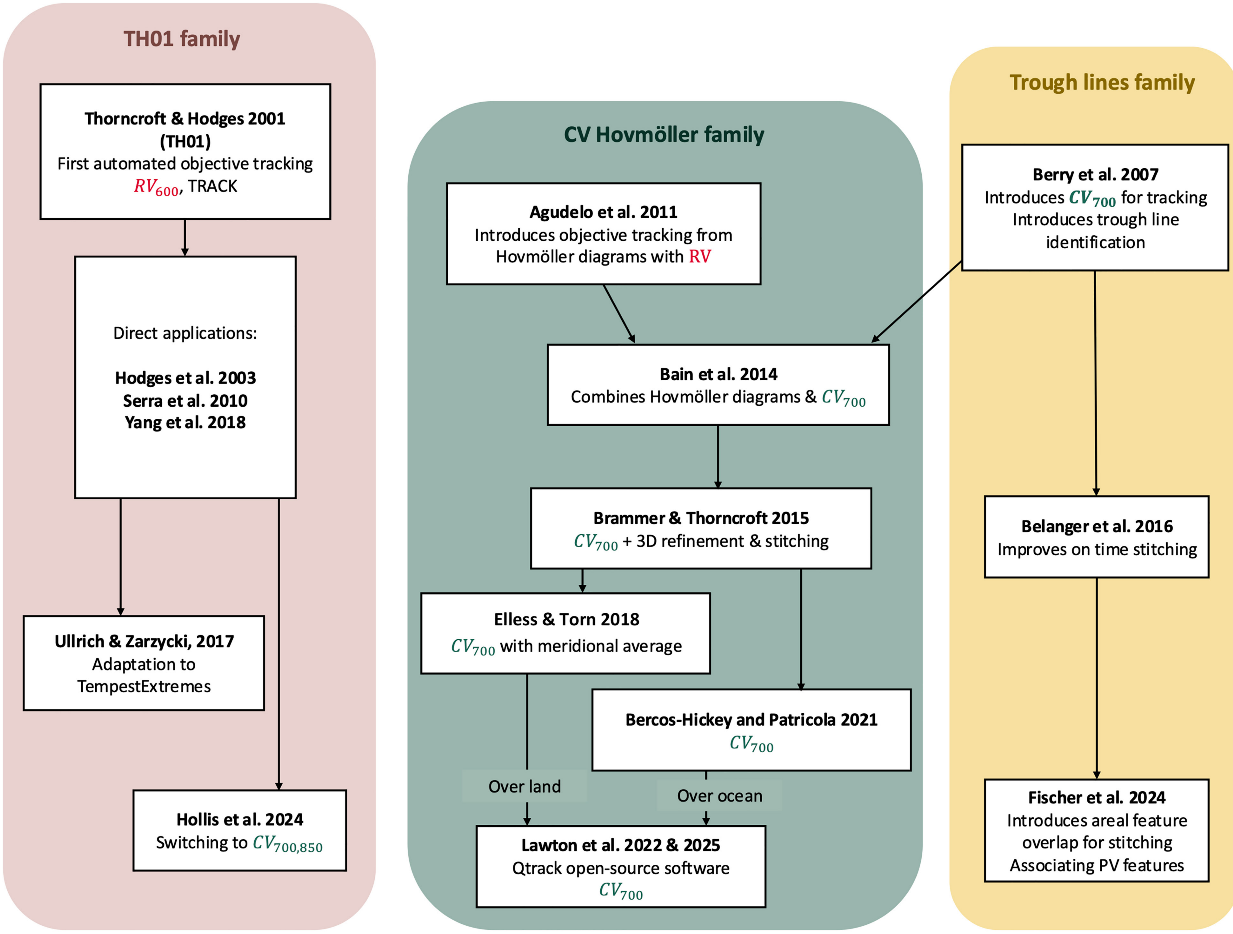

FIG. 10. Evolution of automated AEW trackers across several categories or "families." The subscripts refer to the pressure level of the variables (hPa).

The first automated AEW tracker can be traced back to TH01, who adapted a well-established vortex-tracking algorithm (TRACK; Hodges 1994, 1995, 1999) to the characteristics of AEWs ("TH01 family"; Fig. 10]. TRACK was set up to detect troughs as local maxima in the 600- and 850-hPa relative vorticity (RV) fields on a T42 spectral resolution grid (approximately 300 km at 10°N). Local maxima were then stitched together across time periods by minimizing a cost function for track smoothness. Tracks were further filtered based on predetermined minimum lifetimes (2 days), track length (~1000 km), and vortex strength (0.5×10^{-5} s^{-1}). Several subsequent studies used similar methods, refining the choice of variables [relative vorticity or curvature vorticity (CV)] or smoothing techniques to focus on key features (Hodges et al. 2003; Serra et al. 2010; Yang et al. 2018).

A comparable methodology was implemented within the open-source TempestExtremes feature tracking software (Ullrich and Zarzycki 2017). More recently, Hollis et al. (2024) used TRACK but replaced relative vorticity with curvature vorticity at 700 and 850 hPa, applying specific thresholds to restrict tracked objects to easterly waves, as recommended by Berry et al. (2007). Beyond the TH01 family, Brammer et al. (2018) also demonstrated the benefit of tracking multiple variables across multiple isobaric levels, allowing for structural changes in AEWs and subsequent tropical disturbances while maintaining a coherent feature. This approach, which combines variables across multiple levels and spatial filters, has since been leveraged by Cheng (2019) and Núñez Ocasio et al. (2020b, 2021) to evaluate AEWs across regions and time scales.

Automated vortex tracking routines have the advantage of identifying clear tracks of vortex maxima, performing especially well for strong disturbances or those over the ocean. However, due to the weak synoptic-scale vorticity signature of AEWs and their evolving structure, with numerous short-lived MCSs or vorticity maxima propagating within the synoptic envelope (e.g., Schwendike and Jones 2010; Janiga and Thorncroft 2013), two-dimensional vortex trackers are sensitive to the spatial and temporal resolution of the data and to the filters used to enhance the tracked features.

To address these limitations, automated methods were also developed to combine the benefits of objective vortex tracking with Hovmöller-style analysis ("CV Hovmöller family"; Fig. 10). Agudelo et al. (2011) developed an automated multistep process, similar to Fink and Reiner (2003), by identifying propagating disturbances in relative vorticity across multiple latitude bands and isobaric surfaces, using bandpass-filtered data. Bain et al. (2014) extended this methodology to use curvature vorticity, thereby removing the background shear vorticity and the need for bandpass filtering, to evaluate forecast models' ability to predict AEWs. Brammer and Thorncroft (2015) further refined this method and applied it to 30 years of reanalysis data, focusing on subset wave composites with unfiltered curvature vorticity and adding a latitudinal refinement step to locate the nearest curvature vorticity maxima. This method was modified by Elless and Torn (2018) to more specifically work over the African continent, with Lawton et al. (2022) subsequently combining the Brammer and Thorncroft (2015) steps for overocean tracking and the Elless and Torn (2018) steps for overland tracking in their "QTrack" wave-tracking software. In recent years, multistep tracking methodology has been applied to ensemble forecasts of AEW evolution (Elless and Torn 2018, 2019), climate simulations (Brannan and Martin 2019; Bercos-Hickey and Patricola 2021), AEW interactions with other equatorial waves (Lawton et al. 2022), numerical modeling experiments (Núñez Ocasio et al. 2024), and the relationship between ENSO and AEW characteristics (Lawton et al. 2025).

A notable change in the methodology of tracking AEWs discussed above occurred following Berry et al. (2007). The benefits of curvature vorticity were quickly identified, and it has since been widely adopted as an important field for identifying AEWs (e.g., Bain et al. 2014; Brammer and Thorncroft 2015; Lawton et al. 2022; Hollis et al. 2024). These methods all still rely on either temporal filters, spatial bandpass filters, or spatial averaging to identify disturbances on the AEW scale (2–10 days or 300–1000-km radius). Jonville et al. (2025) recently demonstrated that north and south AEW tracks could be tracked through the choice of bandpass filter applied to the data prior to tracking disturbances, highlighting not only the importance but also dependence on tracking methodology for analysis of the AEW features.

Another family of trackers also emerged from Berry et al. (2007) ("trough line family"; Fig. 10). Belanger et al. (2016) extended trough line analysis into an objective method that stitches trough axes in time. Fischer et al. (2024) further advanced this by adding areal feature overlap and PV feature association to stitch features in time. This approach has the advantage of identifying the trough axis as a two-dimensional feature, rather than reducing it to a point, thereby highlighting trough structure evolution. In a related approach, Downs et al. (2025) developed a deep learning technique to identify tropical easterly wave (TEW) troughs, including AEWs, using satellite and numerical analysis data, based on an archive of subjective TEW analyses from the NHC. Although not trained specifically on AEWs, this method demonstrated skill in identifying wave troughs over western North Africa (west of 0° longitude), and its nonlinear detection framework enhanced the ability to retain trough features across regions.

The choice of temporal or spatial filter, as well as the variable, still influences the tracked disturbance. Different methodologies continue to produce differing individual tracks, but climatological characteristics of the disturbances generally agree. Automated tracking has thus enabled large-scale analyses of the evolution and characteristics of both composite and individual AEWs.

It is important to highlight that the AEW tracks captured by these automated techniques can be highly dependent on the wave-tracking methodology utilized. This is illustrated by the snapshot of AEW tracks presented in Fig. 11, which shows an example from a wave-tracking method in each family tree category and the deep learning tracker developed by Downs et al. (2025). While most AEWs are captured by a majority of the four tracking methods, others are only picked up by a few, and still others vary in the captured lifetime or longitudinal position (Fig. 11a). This is likely related to relative strengths and weaknesses in each tracker's ability to capture AEWs in a given region or of a given strength, as well as differences in the underlying dataset used [e.g., Hollis et al. (2024) use MERRA-2 as opposed to ERA5]. However, even for strong, well-captured waves (e.g., Figs. 11b,c), there are notable differences in the location of the detected wave center.

As such, users of such methods should carefully consider their desired application prior to selecting an objective tracker. This includes the software and data availability, the focus region of an analysis, and the availability of underlying data needed for wave tracking. Furthermore, if using published wave tracks, the source of the tracked data (e.g., the reanalysis or satellite dataset used) and its comparability with a given analysis should be considered. Some AEW trackers have demonstrated enhanced skill in some regions, like Downs et al. (2025) in the Caribbean or Elless and Torn (2018) and Lawton et al. (2022) over the African continent, and many have been more extensively tested on numerical model output than others. To guide these decisions, a summary of tracking characteristics is provided in Table 1, with a more detailed summary available online (see the data availability statement below).

Improvements in open-science practices and resources have created open archives of data and software in recent years. AEW track data from Brammer et al. (2018) combined with MCS data (Núñez Ocasio et al. 2020b, 2021) were made openly available via Núñez Ocasio et al. (2020c,a). Lawton et al. (2022) published both data and software in a community usable package at Lawton (2024). Similar open-science advancements have been made with software and/or data shared openly via online repositories (e.g., Bercos-Hickey 2023; Hollis 2023; Fischer et al. 2023; Downs 2025), as also summarized in Table 1.

5. Future changes to AEW activity and the AEW–AEJ system

Multiple recent studies have examined how AEWs will respond to future warming, although the results are conflicting. Using global climate model (GCM) data, Skinner and Diffenbaugh (2014), Martin and Thorncroft (2015), and Brannan and Martin (2019) found a future increase in AEW activity in the northern wave track, but changes in the southern wave track remained inconclusive, largely owing to poor model resolution of the Guinea Highlands. Hannah and Aiyyer (2017)

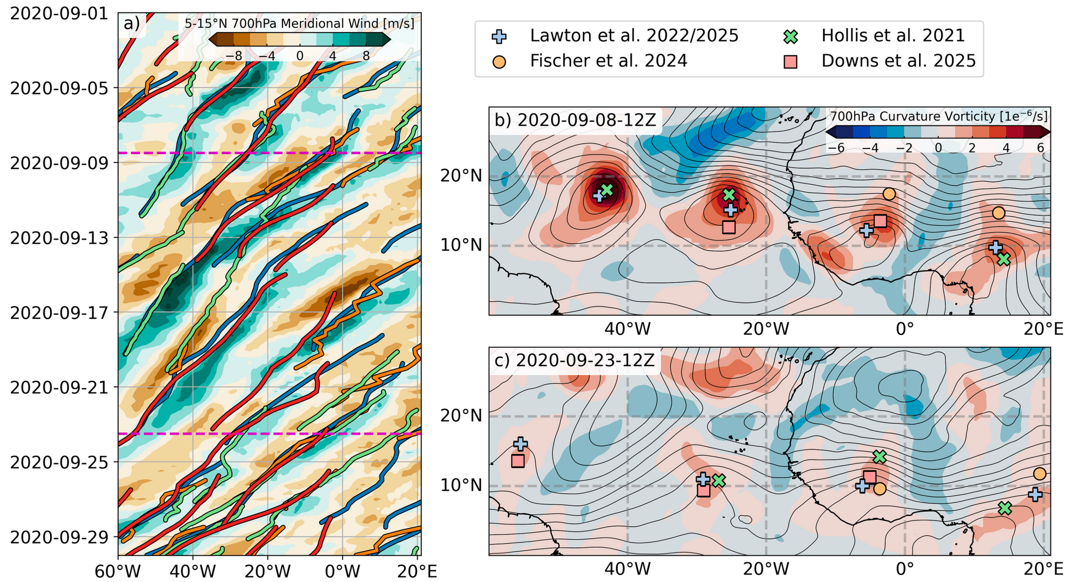

FIG. 11. (a) Example Hovmöller of meridional wind (5°–15°N) and tracks from four open-data AEW track archives: Hollis (2023), Fischer et al. (2023), Downs (2025), and Lawton et al. (2025). (b),(c) CV and streamfunction at 700 hPa for two time periods, with geographic track locations denoted by their respective symbols. Each tracking methodology uses different techniques and fields as summarized in Table 1.

used a superparameterized (type of small explicit model to resolve convection within each grid cell) GCM to examine the response of AEWs to quadrupled carbon dioxide (CO_2) concentrations. They found decreased AEW activity in the southern wave track, which was attributed to increased static stability associated with weak temperature gradient balance, and increased AEW activity in the northern wave track due to enhanced baroclinicity. In contrast to the aforementioned studies, Bercos-Hickey et al. (2023) used three models from the High-Resolution Model Intercomparison Project (HighResMIP) Process-Based Climate Simulation: Advances in High-Resolution Modelling and European Climate Risk Assessments (PRIMAVERA) simulations and found a future increase in the eddy kinetic energy in the regions of the north and south AEW tracks, indicating stronger future AEWs. Similar to Bercos-Hickey et al. (2023), Akinsanola et al. (2025) examined data from multiple CMIP6 models and found a robust increase in AEW activity by the end of the twenty-first century under two future emission scenarios.

Regional climate models have also been used to examine the response of the AEJ and AEWs to climate change, as in Kebe et al. (2020) and Bercos-Hickey and Patricola (2021). Unlike the previous GCM studies, Kebe et al. (2020) found a future decrease in AEW activity and favorable conditions for AEW growth due to a reduction in barotropic and baroclinic instability. Bercos-Hickey and Patricola (2021), however, found a future increase in the number and strength of AEWs due to enhanced baroclinic and barotropic energy conversions and a weaker, northward-shifted AEJ. More recently, using convection-permitting simulations in a limited-area model, Núñez Ocasio and Dougherty (2024) and Núñez Ocasio et al. (2025) reported an intensification of AEWs and a stronger AEJ. Additionally, these novel rainfall-resolving simulations showed enhanced AEW-associated rainfall over land. Disagreement between the aforementioned modeling studies could be due, in part, to the differences in models, model resolution, and wave-tracking methods.

Studies that have examined observational and reanalysis data have also found evidence of changes in AEW activity over time. Historical trends since 1980 indicate an increase in AEW strength as well as a poleward shift of the AEWs (Wang and Gillies 2011; Bercos-Hickey and Patricola-DiRosario 2024; Lawton et al. 2025). Increased AEW activity has also been linked to the observed increasing trend in Atlantic TC activity (Klotzbach et al. 2022; Sobel et al. 2021), with Bercos-Hickey and Patricola-DiRosario (2024) finding that between 1980 and 2022 the increasing trends in Atlantic TC frequency were driven by an increase in TCs with AEW origins, whereas there is no trend in TCs without AEW origins. Together, the future modeling studies and the historical trends in AEW activity demonstrate that the AEJ–AEW system has and will likely continue to be affected by climate change.

6. Summary, challenges, and future directions

a. Short summary

The first scientific accounts of AEWs emerged in the 1930s, when they were linked to North Atlantic hurricanes. Riehl (1945) provided the first depiction of AEWs as westward-propagating synoptic disturbances forming over sub-Saharan Africa during the boreal summer. Since then, understanding has advanced through improved observations and modeling. Early theories emphasized barotropic–baroclinic instabilities in the AEJ, while more recent studies highlight the roles of

TABLE 1. Comparison of select characteristics of AEW trackers, including software and wave track availability. A more detailed table can be found online (http://bit.ly/4pp2CYb). PEW stands for Pacific easterly waves. IR represents the infrared, TCW is the total column water, and q is the specific humidity.

Wave tracker	Algorithm	Tracked features	Regionality	Software availability	Data availability
Thorncroft and Hodges (2001)	TH01	RV_{600}	AEW	TRACK (upon request)	No
Hollis et al. (2024)		$CV_{700,850}$	Global (NH and SH)		MERRA-2
Ullrich and Zarzycki (2017)		RV_{600}		Tempest Extremes	No
Berry et al. (2007)	Trough line identification	Streamfunction CV_{700}	AEW	No	No
Belanger et al. (2016)		2D wind and CV at 600, 700, and 850 hPa	PEW, AEW (NH and SH)	Source code	Reanalysis
Fischer et al. (2024)		CV_{700}	AEW	enstools-feature (Fischer 2023)	ERA5 (Fischer 2023)
Agudelo et al. (2011)	Hovmöller	OLR $RV_{600,700,850,925}$	PEW, AEW	No	No
Bain et al. (2014)		CV_{700}	AEW		
Elless and Torn (2018)			PEW, AEW	Upon request	
Brammer and Thorncroft (2015)	3D tracking		AEW	Source code (Bercos-Hickey 2023)	
Bercos-Hickey and Patricola (2021)					
Lawton et al. (2022, 2025)					
Brammer et al. (2018)		CV, RV, and geopotential height at 700, 850, and 925 hPa	PEW, AEW	Python package QTrack (Lawton 2024)	ERA5 and MERRA-2 (Lawton 2024)
				Upon request	ERA-I via Núñez Ocasio et al. (2020a,c)
Downs et al. (2025)	Deep learning	IR, TCW, q, and 2D wind between 1000 and 550 hPa		Source code and model weights (Downs 2025)	ERA5 (Downs 2025)

moist convection, diabatic heating, and African topography. While there are differences in perspective on whether AEJ instabilities or upscale convective forcing are more dominant to AEW growth and maintenance, these viewpoints have largely been shaped by the observational and modeling resources available at the time. We argue based on the studies reviewed here that both perspectives are complementary.

Summarizing their dynamical features, AEWs are synoptic-scale disturbances that transition from a cold-core structure to a warm-core structure and exhibit both horizontal and vertical tilts—often westward with height—consistent with their baroclinic–barotropic nature. They typically have wavelengths of 2000–6000 km, periods of 3–5 days, and westward speeds of 7–9 m^{-1}. AEWs follow two main tracks: a northern, drier track linked to surface perturbations and a southern, moist track more strongly coupled to the WAM and more associated with downstream TC genesis. Several tracking methods have been developed to study the evolution and trajectories of AEWs. We refer the reader to Table 1 for a summary of the tracking methods reviewed here (section 4), highlighting the specific focus of each approach in the hope that it helps future users select the most appropriate tracker for their research questions. We note that there is a general consensus that most trackers are more sensitive to southern-track AEW characteristics.

AEWs influence rainfall variability, dust transport, and Atlantic hurricane formation. With expanded datasets, recent studies also assess AEW trends under climate change, noting strengthened and poleward-shifted activity since 1980, with projections indicating further intensification in a warming climate.

b. *Outstanding challenges in our understanding of AEWs*

Despite decades of study, major challenges remain, including limited observations over Africa, disagreements about initiation mechanisms of individual AEW cases, and the absence of a standardized AEW observational dataset. These issues are compounded by persistent difficulties in understanding and simulating convection over Africa and its interactions with broader atmospheric processes, including interhemispheric wind flows over western equatorial Africa (Berger et al. 2025), as well as smaller-scale moisture feedback processes coupled with equatorial waves. One of the most pressing gaps is our still-evolving understanding of the role of convection in AEW maintenance and growth. Current mesoscale models, even convection-permitting ones, continue to struggle with accurately predicting AEW initiation, growth, intensity, and propagation, including their uncertainties, related to challenges in initialization and convection schemes (e.g., Elless and Torn 2018; Warner et al. 2023).

Closing the observational gap for AEWs will likely require a combination of targeted field campaigns, advances in satellite observations and retrieval algorithms, and improved in situ observing networks over Africa. Coordinated airborne and ground-based campaigns (e.g., GATE, NAMMA, and CPEX-CV) remain essential for resolving the multiscale interactions between AEWs and convection, particularly during the offshore transition. At the same time, recent advances in geostationary satellite capabilities and retrievals offer new opportunities to better characterize convective and moisture structures over data-sparse regions. However, progress is also limited by sparse surface and upper-air observations and by challenges related to data access and availability, which remain major barriers to comprehensive observational analyses of AEWs.

Advances in high-resolution modeling, artificial intelligence (AI)-based tracking, and improved theories of convection–wave coupling are expected to significantly refine our understanding of AEWs in the coming years. These developments may also help elucidate the underlying processes that differentiate northern-track AEWs from southern-track AEWs or determine whether they represent distinct modes or variations of a single wave structure. They may also provide insight into the relationship between AEWs, MCSs, and localized extreme rainfall events, which are of heightened societal importance.

c. *Future research directions*

While this review was being prepared, deep learning approaches such as using convolutional neural networks (CNNs) have been developed to track AEWs in the broader context of tropical easterly waves (e.g., Downs et al. 2025). Unlike traditional trackers that typically rely on a single variable (such as relative vorticity), the AI-based method can utilize multiple environmental fields (e.g., moisture and winds at multiple levels) to identify wave features. This enables the detection of weaker disturbances—such as those in the Caribbean Sea—that are often missed by conventional approaches due to the weak signature in vorticity fields but can produce significant rainfall and support genesis (e.g., Núñez Ocasio et al. 2026; Herrera 2026) . AI-based trackers could generate long-term, reliable wave datasets with strong potential for operational forecasting applications, especially when large ensembles become available in numerical weather prediction systems. We also note that explainable AI methods such as Shapley additive explanations (SHAP) have the potential to more effectively mimic key environmental factors and dynamical processes controlling AEWs with considering regional variations. Utilizing AI methods may further advance our understanding of underpinning mechanisms for the generation and evolution of AEWs.

The NHC's Tropical Analysis and Forecast Branch (TAFB) routinely monitors AEWs using satellite-derived fields (e.g., precipitable water, motion vectors) and 700-hPa wave tracking from global models (Berry et al. 2007), though this is not an official operational product. These analyses support assessments of downstream tropical cyclone potential. As demand grows for probabilistic TC genesis forecasts (Hon et al. 2023; Conroy et al. 2023), particularly with the increasing use of convection-permitting ensembles, incorporating AEW monitoring into operational early warning systems remains an important and evolving prospect. This includes the evaluation of climate and convection-permitting models in AEW simulations using the knowledge collectively gained above from observations and idealized/regional modeling studies.

As we move into a warmer and moister climate, we are only beginning to understand how these changes will modulate tropical atmospheric dynamics. We hope this review provides future researchers with a foundational and comprehensive starting point for understanding AEWs and helps set the stage to advancing our collective knowledge of how AEWs may evolve in the coming decades.

Acknowledgments. We thank George Kiladis and three anonymous reviewers for their thoughtful feedback during the peer review process. We acknowledge Texas A&M University for supporting the publication of this review. Q. A. L. acknowledges support from the NSF National Center for Atmospheric Research, which is a major facility sponsored by the U.S. National Science Foundation under Cooperative Agreement 1852977. S. B., X. F., and J. S. were supported by the U.K. NERC Large Grant project Huracán (NE/W009587/1). X. F. was also supported by the U.K. National Centre for Atmospheric Science through the NERC National Capability International Programmes Award (NE/X006263/1). This work benefited from the collaborations built during the TROPICANA program at the Institut Pascal (Université Paris-Saclay) with the support of the ANR-11-IDEX-0003-01 Grant.

Data availability statement. No original datasets were generated for this review. A detailed table describing current AEW trackers—an extension of Table 1—can be accessed at http://bit.ly/4pp2CYb. The AEW track data used in this study were obtained from the appropriate source detailed in Table 1. ERA5 data were obtained via the Copernicus Climate Data Store at http://cds.climate.copernicus.eu. The data sources for Fig. 5b are 1) CPEX-CV data (Zawislak et al. 2022), also available through the NASA Global Hydrometeorology Resource Center (GHRC) Distributed Active Archive Center (DAAC) at https://ghrc.nsstc.nasa.gov/home/field-campaigns/cpex-cv, the NASA Atmospheric Science Data Center (ASDC) at https://asdc.larc.nasa.gov/project/CPEX-CV, and the NASA LaRC Suborbital Science Data for Atmospheric Composition at https://www-air.larc.nasa.gov/missions/cpex-cv/index.html; 2) MSG *Meteosat-11* data, available at https://data.eumetsat.int/; 3) GPM IMERG data, available at https://disc.gsfc.nasa.gov/; and 4) the TAMS code to track MCSs, available via Moon and Núñez Ocasio (2025).

REFERENCES

Agudelo, P. A., C. D. Hoyos, J. A. Curry, and P. J. Webster, 2011: Probabilistic discrimination between large-scale environments of intensifying and decaying African easterly waves. *Climate Dyn.*, **36**, 1379–1401, https://doi.org/10.1007/s00382-010-0851-x.

Akinsanola, A. A., A. A. Adebiyi, V. Bobde, O. E. Adeyeri, A. T. Tamoffo, and D. K. Danso, 2025: Projected changes in African easterly wave activity due to climate change. *Commun. Earth Environ.*, **6**, 2, https://doi.org/10.1038/s43247-024-01981-9.

Alaka, G. J., Jr., and E. D. Maloney, 2014: The intraseasonal variability of African easterly wave energetics. *J. Climate*, **27**, 6559–6580, https://doi.org/10.1175/JCLI-D-14-00146.1.

Arnault, J., and F. Roux, 2009: Case study of a developing African easterly wave during NAMMA: An energetic point of view. *J. Atmos. Sci.*, **66**, 2991–3020, https://doi.org/10.1175/2009JAS3009.1.

——, and ——, 2010: Comparison between two case studies of developing and nondeveloping African easterly waves during NAMMA and AMMA/SOP-3: Absolute vertical vorticity budget. *Mon. Wea. Rev.*, **138**, 1420–1445, https://doi.org/10.1175/2009MWR3120.1.

Arnold, J. E., 1966: Easterly wave activity over Africa and in the Atlantic with a note on the intertropical convergence zone during early July, 1961. Department of Geophysical Sciences, University of Chicago, Satellite Meteorology Research Paper 65, 23 pp.

Asaadi, A., G. Brunet, and M. K. Yau, 2017: The importance of critical layer in differentiating developing from nondeveloping easterly waves. *J. Atmos. Sci.*, **74**, 409–417, https://doi.org/10.1175/JAS-D-16-0085.1.

Avila, L. A., R. J. Pasch, and J.-G. Jiing, 2000: Atlantic tropical systems of 1996 and 1997: Years of contrasts. *Mon. Wea. Rev.*, **128**, 3695–3706, https://doi.org/10.1175/1520-0493(2000)128<3695:ATSOAY>2.0.CO;2.

Bain, C. L., K. D. Williams, S. F. Milton, and J. T. Heming, 2014: Objective tracking of African easterly waves in Met Office models. *Quart. J. Roy. Meteor. Soc.*, **140**, 47–57, https://doi.org/10.1002/qj.2110.

Belanger, J. I., M. T. Jelinek, and J. A. Curry, 2016: A climatology of easterly waves in the tropical Western Hemisphere. *Geosci. Data J.*, **3**, 40–49, https://doi.org/10.1002/gdj3.40.

Bercos-Hickey, E., 2023: African easterly wave tracking algorithm v1.0. GitHub, accessed 24 September 2025, https://github.com/mehtut/AEW_Tracker.

——, and C. M. Patricola, 2021: Anthropogenic influences on the African easterly jet–African easterly wave system. *Climate Dyn.*, **57**, 2779–2792, https://doi.org/10.1007/s00382-021-05838-1.

——, and C. M. Patricola-DiRosario, 2024: Characteristics and trends of Atlantic tropical cyclones that do and do not develop from African easterly waves. *Quart. J. Roy. Meteor. Soc.*, **150**, 4951–4968, https://doi.org/10.1002/qj.4850.

——, and C. M. Patricola, 2025: Drivers of Atlantic tropical cyclogenesis: African easterly waves and the environment. *Geophys. Res. Lett.*, **52**, e2024GL112002, https://doi.org/10.1029/2024GL112002.

——, T. R. Nathan, and S.-H. Chen, 2017: Saharan dust and the African easterly jet–African easterly wave system: Structure, location and energetics. *Quart. J. Roy. Meteor. Soc.*, **143**, 2797–2808, https://doi.org/10.1002/qj.3128.

——, ——, and ——, 2020: On the relationship between the African easterly jet, Saharan mineral dust aerosols, and West African precipitation. *J. Climate*, **33**, 3533–3546, https://doi.org/10.1175/JCLI-D-18-0661.1.

——, ——, and ——, 2022: Effects of Saharan dust aerosols and West African precipitation on the energetics of African easterly waves. *J. Atmos. Sci.*, **79**, 1911–1926, https://doi.org/10.1175/JAS-D-21-0157.1.

——, C. M. Patricola, B. Loring, and W. D. Collins, 2023: The relationship between African easterly waves and tropical cyclones in historical and future climates in the HighResMIP-PRIMAVERA simulations. *J. Geophys. Res. Atmos.*, **128**, e2022JD037471, https://doi.org/10.1029/2022JD037471.

Berger, A., P. Camberlin, J. Pergaud, Y. Bahuet-Bourret, R. Aellig, and O. Champagne, 2025: The dry-season low-level cloud cover over western equatorial Africa: A case study with a mesoscale atmospheric model. *Quart. J. Roy. Meteor. Soc.*, **151**, e4962, https://doi.org/10.1002/qj.4962.

Berry, G., C. Thorncroft, and T. Hewson, 2007: African easterly waves during 2004—Analysis using objective techniques. *Mon. Wea. Rev.*, **135**, 1251–1267, https://doi.org/10.1175/MWR3343.1.

Berry, G. J., and C. Thorncroft, 2005: Case study of an intense African easterly wave. *Mon. Wea. Rev.*, **133**, 752–766, https://doi.org/10.1175/MWR2884.1.

——, and C. D. Thorncroft, 2012: African easterly wave dynamics in a mesoscale numerical model: The upscale role of convection. *J. Atmos. Sci.*, **69**, 1267–1283, https://doi.org/10.1175/JAS-D-11-099.1.

Brammer, A., and C. D. Thorncroft, 2015: Variability and evolution of African easterly wave structures and their relationship with tropical cyclogenesis over the eastern Atlantic. *Mon. Wea. Rev.*, **143**, 4975–4995, https://doi.org/10.1175/MWR-D-15-0106.1.

——, and ——, 2017: Spatial and temporal variability of the three-dimensional flow around African easterly waves. *Mon. Wea. Rev.*, **145**, 2879–2895, https://doi.org/10.1175/MWR-D-16-0454.1.

——, ——, and J. P. Dunion, 2018: Observations and predictability of a nondeveloping tropical disturbance over the eastern Atlantic. *Mon. Wea. Rev.*, **146**, 3079–3096, https://doi.org/10.1175/MWR-D-18-0065.1.

Brannan, A. L., and E. R. Martin, 2019: Future characteristics of African easterly wave tracks. *Climate Dyn.*, **52**, 5567–5584, https://doi.org/10.1007/s00382-018-4465-z.

Burpee, R. W., 1972: The origin and structure of easterly waves in the lower troposphere of North Africa. *J. Atmos. Sci.*, **29**, 77–90, https://doi.org/10.1175/1520-0469(1972)029<0077:TOASOE>2.0.CO;2.

——, 1974: Characteristics of North African easterly waves during the summers of 1968 and 1969. *J. Atmos. Sci.*, **31**, 1556–1570, https://doi.org/10.1175/1520-0469(1974)031<1556:CONAEW>2.0.CO;2.

Carlson, T. N., 1969a: Some remarks on African disturbances and their progress over the tropical Atlantic. *Mon. Wea. Rev.*, **97**, 716–726, https://doi.org/10.1175/1520-0493(1969)097<0716:SROADA>2.3.CO;2.

——, 1969b: Synoptic histories of three African disturbances that developed into Atlantic hurricanes. *Mon. Wea. Rev.*, **97**, 256–276, https://doi.org/10.1175/1520-0493(1969)097<0256:SHOTAD>2.3.CO;2.

Charney, J. G., and M. E. Stern, 1962: On the stability of internal baroclinic jets in a rotating atmosphere. *J. Atmos. Sci.*, **19**, 159–172, https://doi.org/10.1175/1520-0469(1962)019<0159:OTSOIB>2.0.CO;2.

Chen, T.-C., 2006: Characteristics of African easterly waves depicted by ECMWF reanalyses for 1991–2000. *Mon. Wea. Rev.*, **134**, 3539–3566, https://doi.org/10.1175/MWR3259.1.

——, S.-Y. Wang, and A. J. Clark, 2008: North Atlantic hurricanes contributed by African easterly waves north and south of the African easterly jet. *J. Climate*, **21**, 6767–6776, https://doi.org/10.1175/2008JCLI2523.1.

Cheng, Y.-M., 2019: Variability of African easterly waves. Ph.D. thesis, University at Albany, State University of New York, 187 pp., https://doi.org/10.54014/R63S-6XXD.

——, C. D. Thorncroft, and G. N. Kiladis, 2019: Two contrasting African easterly wave behaviors. *J. Atmos. Sci.*, **76**, 1753–1768, https://doi.org/10.1175/JAS-D-18-0300.1.

Conroy, A., and Coauthors, 2023: Track forecast: Operational capability and new techniques - summary from the Tenth International Workshop on Tropical Cyclones (IWTC-10). *Trop. Cyclone Res. Rev.*, **12**, 64–80, https://doi.org/10.1016/j.tcrr.2023.05.002.

Cornforth, R., and Coauthors, 2017: Synoptic systems. *Meteorology of Tropical West Africa: The Forecasters' Handbook*, D. J. Parker and M. Diop-Kane, Eds., Wiley, 40–89.

Cornforth, R. J., and B. J. Hoskins, 2009: Understanding African easterly waves: A moist singular vector approach. *Atmos. Sci. Lett.*, **10**, 185–191, https://doi.org/10.1002/asl.231.

Crétat, J., E. K. Vizy, and K. H. Cook, 2015: The relationship between African easterly waves and daily rainfall over West Africa: Observations and regional climate simulations. *Climate Dyn.*, **44**, 385–404, https://doi.org/10.1007/s00382-014-2120-x.

Delany, A. C., A. Claire Delany, D. W. Parkin, J. J. Griffin, E. D. Goldberg, and B. E. F. Reimann, 1967: Airborne dust collected at Barbados. *Geochim. Cosmochim. Acta*, **31**, 885–909, https://doi.org/10.1016/S0016-7037(67)80037-1.

Desbois, M., T. Kayiranga, B. Gnamien, S. Guessous, and L. Picon, 1988: Characterization of some elements of the Sahelian climate and their interannual variations for July 1983, 1984 and 1985 from the analysis of METEOSAT ISCCP data. *J. Climate*, **1**, 867–904, https://doi.org/10.1175/1520-0442(1988)001<0867:COSEOT>2.0.CO;2.

Diedhiou, A., S. Janicot, A. Viltard, P. de Felice, and H. Laurent, 1999: Easterly wave regimes and associated convection over West Africa and tropical Atlantic: Results from the NCEP/NCAR and ECMWF reanalyses. *Climate Dyn.*, **15**, 795–822, https://doi.org/10.1007/s003820050316.

——, ——, ——, and P. de Félice, 2002: Energetics of easterly wave disturbances over West Africa and the tropical Atlantic: A climatology from the 1979–95 NCEP/NCAR reanalyses. *Climate Dyn.*, **18**, 487–500, https://doi.org/10.1007/s00382-001-0195-7.

Downs, W., 2025: Tropical easterly wave, ITCZ, and monsoon trough identification using neural networks. Open Science Framework, accessed 24 September 2025, https://osf.io/hk73a/.

Downs, W. B., S. J. Majumdar, and A. D. Mahoney, 2025: Using deep learning to identify tropical easterly waves, the intertropical convergence zone, and the monsoon trough. *Mon. Wea. Rev.*, **153**, 1581–1604, https://doi.org/10.1175/MWR-D-24-0195.1.

Dunn, G. E., 1940: Cyclogenesis in the tropical Atlantic. *Bull. Amer. Meteor. Soc.*, **21**, 215–229, https://doi.org/10.1175/1520-0477-21.6.215.

——, 1962: The hurricane season of 1961. *Mon. Wea. Rev.*, **90**, 107–119, https://doi.org/10.1175/1520-0493(1962)090<0107:THSO>2.0.CO;2.

Duvel, J. P., 1990: Convection over tropical Africa and the Atlantic Ocean during northern summer. Part II: Modulation by easterly waves. *Mon. Wea. Rev.*, **118**, 1855–1868, https://doi.org/10.1175/1520-0493(1990)118<1855:COTAAT>2.0.CO;2.

Duvel, J.-P., 2021: On vortices initiated over West Africa and their impact on North Atlantic tropical cyclones. *Mon. Wea. Rev.*, **149**, 585–601, https://doi.org/10.1175/MWR-D-20-0252.1.

Elless, T. J., and R. D. Torn, 2018: African easterly wave forecast verification and its relation to convective errors within the ECMWF ensemble prediction system. *Wea. Forecasting*, **33**, 461–477, https://doi.org/10.1175/WAF-D-17-0130.1.

——, and ——, 2019: Investigating the factors that contribute to African easterly wave intensity forecast uncertainty in the ECMWF ensemble prediction system. *Mon. Wea. Rev.*, **147**, 1679–1698, https://doi.org/10.1175/MWR-D-18-0071.1.

Emanuel, K., 2003: Tropical cyclones. *Annu. Rev. Earth Planet. Sci.*, **31**, 75–104, https://doi.org/10.1146/annurev.earth.31.100901.141259.

——, 2026: *Physics of the Tropical Atmosphere and Tropical Cyclones.* Princeton University Press, 704 pp.

Engel, T., A. H. Fink, P. Knippertz, G. Pante, and J. Bliefernicht, 2017: Extreme precipitation in the West African cities of Dakar and Ouagadougou: Atmospheric dynamics and implications for flood risk assessments. *J. Hydrometeor.*, **18**, 2937–2957, https://doi.org/10.1175/JHM-D-16-0218.1.

Erickson, C. O., 1963: An incipient hurricane near the West African coast. *Mon. Wea. Rev.*, **91**, 61–68, https://doi.org/10.1175/1520-0493(1963)091<0061:AIHNTW>2.3.CO;2.

Fink, A. H., and A. Reiner, 2003: Spatiotemporal variability of the relation between African easterly waves and West African squall lines in 1998 and 1999. *J. Geophys. Res.*, **108**, 4332, https://doi.org/10.1029/2002JD002816.

Fischer, C., 2023: Enstools-feature: A framework for identification and tracking of meteorological features. Zenodo, https://doi.org/10.5281/zenodo.10062273.

——, A. H. Fink, E. Schömer, M. Riemer, and M. Rautenhaus, 2023: AEWDAT - African easterly waves: Identified and tracked wave troughs. Zenodo, accessed 24 September 2025, https://doi.org/10.5281/zenodo.8403744.

——, ——, ——, M. Rautenhaus, and M. Riemer, 2024: An objective identification technique for potential vorticity structures associated with African easterly waves. *Geosci. Model Dev.*, **17**, 4213–4228, https://doi.org/10.5194/gmd-17-4213-2024.

Gray, W. M., 1968: Global view of the origin of tropical disturbances and storms. *Mon. Wea. Rev.*, **96**, 669–700, https://doi.org/10.1175/1520-0493(1968)096<0669:GVOTOO>2.0.CO;2.

Grogan, D. F. P., T. R. Nathan, and S.-H. Chen, 2016: Effects of Saharan dust on the linear dynamics of African easterly waves. *J. Atmos. Sci.*, **73**, 891–911, https://doi.org/10.1175/JAS-D-15-0143.1.

Hall, N. M. J., G. N. Kiladis, and C. D. Thorncroft, 2006: Three-dimensional structure and dynamics of African easterly waves. Part II: Dynamical modes. *J. Atmos. Sci.*, **63**, 2231–2245, https://doi.org/10.1175/JAS3742.1.

Hamilton, H. L., G. S. Young, J. L. Evans, J. D. Fuentes, and K. M. Núñez Ocasio, 2017: The relationship between the Guinea Highlands and the West African offshore rainfall maximum. *Geophys. Res. Lett.*, **44**, 1158–1166, https://doi.org/10.1002/2016GL071170.

——, K. M. Núñez Ocasio, J. L. Evans, G. S. Young, and J. D. Fuentes, 2020: Topographic influence on the African easterly jet and African easterly wave energetics. *J. Geophys. Res. Atmos.*, **125**, e2019JD032138, https://doi.org/10.1029/2019JD032138.

Hankes, I., Z. Wang, G. Zhang, and C. Fritz, 2015: Merger of African easterly waves and formation of Cape Verde storms. *Quart. J. Roy. Meteor. Soc.*, **141**, 1306–1319, https://doi.org/10.1002/qj.2439.

Hannah, W. M., and A. Aiyyer, 2017: Reduced African easterly wave activity with quadrupled CO_2 in the superparameterized CESM. *J. Climate*, **30**, 8253–8274, https://doi.org/10.1175/JCLI-D-16-0822.1.

Hayashi, Y., 1982: Space-time spectral analysis and its applications to atmospheric waves. *J. Meteor. Soc. Japan*, **60**, 156–171, https://doi.org/10.2151/jmsj1965.60.1_156.

Herrera, D. A., and Coauthors, 2026: Assessing the role of tropical cyclones on drought characteristics in the hurricane region of the Americas between 1983 and 2024. *J. Geophys. Res. Atmos.*, **131**, e2025JD045998, https://doi.org/10.1029/2025JD045998.

Hersbach, H., and Coauthors, 2020: The ERA5 global reanalysis. *Quart. J. Roy. Meteor. Soc.*, **146**, 1999–2049, https://doi.org/10.1002/qj.3803.

Hill, C. M., and Y.-L. Lin, 2003: Initiation of a mesoscale convective complex over the Ethiopian Highlands preceding the genesis of Hurricane Alberto (2000). *Geophys. Res. Lett.*, **30**, 1232, https://doi.org/10.1029/2002GL016655.

Hodges, K. I., 1994: A general method for tracking analysis and its application to meteorological data. *Mon. Wea. Rev.*, **122**, 2573–2586, https://doi.org/10.1175/1520-0493(1994)122<2573:AGMFTA>2.0.CO;2.

——, 1995: Feature tracking on the unit sphere. *Mon. Wea. Rev.*, **123**, 3458–3465, https://doi.org/10.1175/1520-0493(1995)123<3458:FTOTUS>2.0.CO;2.

——, 1999: Adaptive constraints for feature tracking. *Mon. Wea. Rev.*, **127**, 1362–1373, https://doi.org/10.1175/1520-0493(1999)127<1362:ACFFT>2.0.CO;2.

——, B. J. Hoskins, J. Boyle, and C. Thorncroft, 2003: A comparison of recent reanalysis datasets using objective feature tracking: Storm tracks and tropical easterly waves. *Mon. Wea. Rev.*, **131**, 2012–2037, https://doi.org/10.1175/1520-0493(2003)131<2012:ACORRD>2.0.CO;2.

Hollis, M. A., 2023: A global climatology of tropical easterly waves. Zenodo, accessed 24 September 2025, https://doi.org/10.5281/zenodo.10076724.

——, R. R. McCrary, J. P. Stachnik, C. Lewis-Merritt, and E. R. Martin, 2024: A global climatology of tropical easterly waves. *Climate Dyn.*, **62**, 2317–2332, https://doi.org/10.1007/s00382-023-07025-w.

Hon, K. K., and Coauthors, 2023: Recent advances in operational tropical cyclone genesis forecast. *Trop. Cyclone Res. Rev.*, **12**, 323–340, https://doi.org/10.1016/j.tcrr.2023.12.001.

Hopsch, S. B., C. D. Thorncroft, K. Hodges, and A. Aiyyer, 2007: West African storm tracks and their relationship to Atlantic tropical cyclones. *J. Climate*, **20**, 2468–2483, https://doi.org/10.1175/JCLI4139.1.

——, ——, and K. R. Tyle, 2010: Analysis of African easterly wave structures and their role in influencing tropical cyclogenesis. *Mon. Wea. Rev.*, **138**, 1399–1419, https://doi.org/10.1175/2009MWR2760.1.

Houze, R. A., Jr., 2004: Mesoscale convective systems. *Rev. Geophys.*, **42**, RG4003, https://doi.org/10.1029/2004RG000150.

Hovmöller, E., 1949: The trough-and-ridge diagram. *Tellus*, **1** (2), 62–66, https://doi.org/10.3402/tellusa.v1i2.8498.

Hsieh, J.-S., and K. H. Cook, 2005: Generation of African easterly wave disturbances: Relationship to the African easterly jet. *Mon. Wea. Rev.*, **133**, 1311–1327, https://doi.org/10.1175/MWR2916.1.

——, and ——, 2007: A study of the energetics of African easterly waves using a regional climate model. *J. Atmos. Sci.*, **64**, 421–440, https://doi.org/10.1175/JAS3851.1.

——, and ——, 2008: On the instability of the African easterly jet and the generation of African waves: Reversals of the potential vorticity gradient. *J. Atmos. Sci.*, **65**, 2130–2151, https://doi.org/10.1175/2007JAS2552.1.

Hubert, H., 1939: Origine Africaine d'un cyclone tropical Atlantique. *Ann. Phys. Globe France d'Outre-Mer*, **6**, 97–115.

Huffman, G. J., D. T. Bolvin, E. J. Nelkin, and J. Tan, 2019: Integrated Multi-satellitE Retrievals for GPM (IMERG) technical documentation. IMERG Tech. Doc., 77 pp., https://gpm.nasa.gov/sites/default/files/document_files/IMERG_doc_190909.pdf.

Janiga, M. A., and C. D. Thorncroft, 2013: Regional differences in the kinematic and thermodynamic structure of African easterly waves. *Quart. J. Roy. Meteor. Soc.*, **139**, 1598–1614, https://doi.org/10.1002/qj.2047.

——, and ——, 2016: The influence of African easterly waves on convection over tropical Africa and the East Atlantic. *Mon. Wea. Rev.*, **144**, 171–192, https://doi.org/10.1175/MWR-D-14-00419.1.

Jenney, A. M., R. A. Houze Jr., M. LeMone, E. J. Thompson, K. M. Núñez Ocasio, C. Zhang, and T. R. Nathan, 2025: Celebrating 50 years since GATE. *Bull. Amer. Meteor. Soc.*, **106**, E576–E595, https://doi.org/10.1175/BAMS-D-24-0063.1.

Jiang, X., H. Su, S. S. Chen, and P. A. Ullrich, 2023: Simulation of African easterly waves in a global climate model. *J. Climate*, **36**, 1415–1433, https://doi.org/10.1175/JCLI-D-22-0090.1.

Jonville, T., C. Flamant, and C. Lavaysse, 2024: Dynamical study of three African easterly waves in September 2021. *Quart. J. Roy. Meteor. Soc.*, **150**, 2489–2509, https://doi.org/10.1002/qj.4720.

——, E. Cornillault, C. Lavaysse, P. Peyrillé, and C. Flamant, 2025: Distinguishing North and South African easterly waves with a spectral method: Implication for tropical cyclogenesis from mergers in the North Atlantic. *Quart. J. Roy. Meteor. Soc.*, **151**, e4909, https://doi.org/10.1002/qj.4909.

Kebe, I., I. Diallo, M. B. Sylla, F. De Sales, and A. Diedhiou, 2020: Late 21st century projected changes in the relationship between precipitation, African easterly jet, and African easterly waves. *Atmosphere*, **11**, 353, https://doi.org/10.3390/atmos11040353.

Kerns, B., K. Greene, and E. Zipser, 2008: Four years of tropical ERA-40 vorticity maxima tracks. Part I: Climatology and vertical vorticity structure. *Mon. Wea. Rev.*, **136**, 4301–4319, https://doi.org/10.1175/2008MWR2390.1.

Kiladis, G. N., C. D. Thorncroft, and N. M. J. Hall, 2006: Three-dimensional structure and dynamics of African easterly waves. Part I: Observations. *J. Atmos. Sci.*, **63**, 2212–2230, https://doi.org/10.1175/JAS3741.1.

——, M. C. Wheeler, P. T. Haertel, K. H. Straub, and P. E. Roundy, 2009: Convectively coupled equatorial waves. *Rev. Geophys.*, **47**, RG2003, https://doi.org/10.1029/2008RG000266.

Klotzbach, P. J., K. M. Wood, C. J. Schreck III, S. G. Bowen, C. M. Patricola, and M. M. Bell, 2022: Trends in global tropical cyclone activity: 1990–2021. *Geophys. Res. Lett.*, **49**, e2021GL095774, https://doi.org/10.1029/2021GL095774.

Knippertz, P., and Coauthors, 2022: The intricacies of identifying equatorial waves. *Quart. J. Roy. Meteor. Soc.*, **148**, 2814–2852, https://doi.org/10.1002/qj.4338.

Kuang, Z., 2008: A moisture-stratiform instability for convectively coupled waves. *J. Atmos. Sci.*, **65**, 834–854, https://doi.org/10.1175/2007JAS2444.1.

Lafore, J.-P., and Coauthors, 2017: A multi-scale analysis of the extreme rain event of Ouagadougou in 2009. *Quart. J. Roy. Meteor. Soc.*, **143**, 3094–3109, https://doi.org/10.1002/qj.3165.

Laing, A. G., R. Carbone, V. Levizzani, and J. Tuttle, 2008: The propagation and diurnal cycles of deep convection in northern tropical Africa. *Quart. J. Roy. Meteor. Soc.*, **134**, 93–109, https://doi.org/10.1002/qj.194.

Landsea, C. W., 1993: A climatology of intense (or major) Atlantic hurricanes. *Mon. Wea. Rev.*, **121**, 1703–1713, https://doi.org/10.1175/1520-0493(1993)121<1703:ACOIMA>2.0.CO;2.

Lau, K.-H., and N.-C. Lau, 1992: The energetics and propagation dynamics of tropical summertime synoptic-scale disturbances. *Mon. Wea. Rev.*, **120**, 2523–2539, https://doi.org/10.1175/1520-0493(1992)120<2523:TEAPDO>2.0.CO;2.

Lawton, Q., 2024: Objective African easterly tracks in reanalysis data using "Qtrack". Zenodo, accessed 15 September 2025, https://doi.org/10.5281/zenodo.13350859.

Lawton, Q. A., and S. J. Majumdar, 2023: Convectively coupled Kelvin waves and tropical cyclogenesis: Connections through convection and moisture. *Mon. Wea. Rev.*, **151**, 1647–1666, https://doi.org/10.1175/MWR-D-23-0005.1.

——, ——, K. Dotterer, C. Thorncroft, and C. J. Schreck III, 2022: The influence of convectively coupled Kelvin waves on African easterly waves in a wave-following framework. *Mon. Wea. Rev.*, **150**, 2055–2072, https://doi.org/10.1175/MWR-D-21-0321.1.

——, B. Weiser, and S. J. Majumdar, 2025: On the interannual variability of African easterly waves and its relationship with El Niño–Southern Oscillation. *J. Climate*, **38**, 5791–5808, https://doi.org/10.1175/JCLI-D-25-0113.1.

Leppert, K. D., II, D. J. Cecil, and W. A. Petersen, 2013: Relation between tropical easterly waves, convection, and tropical cyclogenesis: A Lagrangian perspective. *Mon. Wea. Rev.*, **141**, 2649–2668, https://doi.org/10.1175/MWR-D-12-00217.1.

Lin, Y.-L., L. Liu, G. Tang, J. Spinks, and W. Jones, 2013: Origin of the pre-tropical storm Debby (2006) African easterly wave-mesoscale convective system. *Meteor. Atmos. Phys.*, **120**, 123–144, https://doi.org/10.1007/s00703-013-0248-6.

Lorenz, E. N., 1955: Available potential energy and the maintenance of the general circulation. *Tellus*, **7** (2), 157–167, https://doi.org/10.1111/j.2153-3490.1955.tb01148.x.

Lubis, S. W., and C. Jacobi, 2015: The modulating influence of convectively coupled equatorial waves (CCEWs) on the variability of tropical precipitation. *Int. J. Climatol.*, **35**, 1465–1483, https://doi.org/10.1002/joc.4069.

Madden, R. A., and P. R. Julian, 1971: Detection of a 40–50 day oscillation in the zonal wind in the tropical Pacific. *J. Atmos. Sci.*, **28**, 702–708, https://doi.org/10.1175/1520-0469(1971)028<0702:DOADOI>2.0.CO;2.

Maloney, E. D., and C. Zhang, 2016: Dr. Yanai's contributions to the discovery and science of the MJO. *Multiscale Convection-Coupled Systems in the Tropics: A tribute to Dr. Michio Yanai, Meteor. Monogr.*, No. 56, Amer. Meteor. Soc., https://doi.org/10.1175/AMSMONOGRAPHS-D-15-0003.1.

Mapes, B. E., 2000: Convective inhibition, subgrid-scale triggering energy, and stratiform instability in a toy tropical wave model. *J. Atmos. Sci.*, **57**, 1515–1535, https://doi.org/10.1175/1520-0469(2000)057<1515:CISSTE>2.0.CO;2.

Maranan, M., A. H. Fink, P. Knippertz, S. D. Francis, A. B. Akpo, G. Jegede, and C. Yorke, 2019: Interactions between convection and a moist vortex associated with an extreme rainfall event over southern West Africa. *Mon. Wea. Rev.*, **147**, 2309–2328, https://doi.org/10.1175/MWR-D-18-0396.1.

Martes, R. M. V., Á. F. Adames Corraliza, and V. C. Mayta, 2023: The role of water vapor and temperature in the thermodynamics of tropical northeast Pacific and African easterly waves. *J. Atmos. Sci.*, **80**, 2305–2322, https://doi.org/10.1175/JAS-D-22-0177.1.

Martin, E. R., and C. Thorncroft, 2015: Representation of African easterly waves in CMIP5 models. *J. Climate*, **28**, 7702–7715, https://doi.org/10.1175/JCLI-D-15-0145.1.

Martinez, G., A. Rowe, K. M. Núñez Ocasio, Z. L. Moon, and B. Rodenkirch, 2025: Evaluating environmental moisture relative to tropical deep convective growth using CPEX-CV airborne and satellite observations. *J. Geophys. Res. Atmos.*, **130**, e2025JD043877, https://doi.org/10.1029/2025JD043877.

Mathon, V., H. Laurent, and T. Lebel, 2002: Mesoscale convective system rainfall in the Sahel. *J. Appl. Meteor.*, **41**, 1081–1092, https://doi.org/10.1175/1520-0450(2002)041<1081:MCSRIT>2.0.CO;2.

Mayta, V. C., Á. F. Adames Corraliza, Q.-J. Lin, and R. M. Vargas Martes, 2025a: Caribbean easterly waves: Structure, thermodynamics, and instability mechanisms. *J. Atmos. Sci.*, **82**, 1451–1465, https://doi.org/10.1175/JAS-D-24-0232.1.

——, ——, K. T. Maldonado, H. Luo, and K. M. Núñez Ocasio, 2025b: Thermodynamic processes governing the evolution of developing and strong nondeveloping African easterly waves. *J. Atmos. Sci.*, **82**, 1161–1174, https://doi.org/10.1175/JAS-D-24-0125.1.

Mekonnen, A., C. D. Thorncroft, and A. R. Aiyyer, 2006: Analysis of convection and its association with African easterly waves. *J. Climate*, **19**, 5405–5421, https://doi.org/10.1175/JCLI3920.1.

Moon, Z., and K. M. Núñez Ocasio, 2025: knubez/TAMS: v 0.1.6 (v0.1.6). Zenodo, https://doi.org/10.5281/zenodo.14624956.

Muench, H. S., 1965: On the dynamics of the wintertime stratosphere circulation. *J. Atmos. Sci.*, **22**, 349–360, https://doi.org/10.1175/1520-0469(1965)022<0349:OTDOTW>2.0.CO;2.

Nam, C. C., M. M. Bell, and D. Tao, 2023: Bifurcation points for tropical cyclone genesis and intensification in sheared and dry environments. *J. Atmos. Sci.*, **80**, 2239–2259, https://doi.org/10.1175/JAS-D-22-0100.1.

Nicholls, S. D., and K. I. Mohr, 2010: An analysis of the environments of intense convective systems in West Africa in 2003. *Mon. Wea. Rev.*, **138**, 3721–3739, https://doi.org/10.1175/2010MWR3321.1.

Nicholson, S. E., 2009: On the factors modulating the intensity of the tropical rainbelt over West Africa. *Int. J. Climatol.*, **29**, 673–689, https://doi.org/10.1002/joc.1702.

Nitta, T., and Y. Takayabu, 1985: Global analysis of the lower tropospheric disturbances in the tropics during the northern summer of the FGGE year part II: Regional characteristics of the disturbances. *Pure Appl. Geophys.*, **123**, 272–292, https://doi.org/10.1007/BF00877023.

NOAA, 2015: 75th anniversary of Gordon Dunn's "isallobaric waves" paper. NOAA Atlantic Oceanographic and Meteorological Laboratory Hurricane Blog, accessed 25 June 2025, https://www.aoml.noaa.gov/hurricane_blog/75th-anniversary-of-gordon-dunns-isallobaric-waves-paper/.

Norquist, D. C., E. E. Recker, and R. J. Reed, 1977: The energetics of African wave disturbances as observed during phase III of GATE. *Mon. Wea. Rev.*, **105**, 334–342, https://doi.org/10.1175/1520-0493(1977)105<0334:TEOAWD>2.0.CO;2.

Nowottnick, E. P., and Coauthors, 2024: Dust, convection, winds, and waves: The 2022 NASA CPEX-CV campaign. *Bull. Amer. Meteor. Soc.*, **105**, E2097–E2125, https://doi.org/10.1175/BAMS-D-23-0201.1.

Núñez Ocasio, K. M., and R. Rios-Berrios, 2023: African easterly wave evolution and tropical cyclogenesis in a pre-Helene (2006) hindcast using the Model for Prediction Across Scales-Atmosphere (MPAS-A). *J. Adv. Model. Earth Syst.*, **15**, e2022MS003181, https://doi.org/10.1029/2022MS003181.

——, and Z. L. Moon, 2024: TAMS: A tracking, classifying, and variable-assigning algorithm for mesoscale convective systems in simulated and satellite-derived datasets. *Geosci. Model Dev.*, **17**, 6035–6049, https://doi.org/10.5194/gmd-17-6035-2024.

——, and E. M. Dougherty, 2024: The effect of pseudo-global warming on the weather-climate system of Africa in a convection-permitting model. *Geophys. Res. Lett.*, **51**, e2024GL112341, https://doi.org/10.1029/2024GL112341.

——, A. Brammer, J. L. Evans, G. S. Young, and Z. L. Moon, 2020a: Favorable monsoon environment over eastern Africa for subsequent tropical cyclogenesis of African easterly waves. datacommons@psu, accessed 12 September 2025, https://doi.org/10.26208/fms6-p713.

——, J. L. Evans, and G. S. Young, 2020b: A wave-relative framework analysis of AEW–MCS interactions leading to tropical cyclogenesis. *Mon. Wea. Rev.*, **148**, 4657–4671, https://doi.org/10.1175/MWR-D-20-0152.1.

——, ——, and ——, 2020c: A wave-relative framework analysis of AEW-MCS interactions leading to tropical cyclogenesis. datacommons@psu, accessed 12 September 2025, https://doi.org/10.26208/frz9-7t95.

——, ——, and ——, 2020d: Tracking mesoscale convective systems that are potential candidates for tropical cyclogenesis. *Mon. Wea. Rev.*, **148**, 655–669, https://doi.org/10.1175/MWR-D-19-0070.1.

——, A. Brammer, J. L. Evans, G. S. Young, and Z. L. Moon, 2021: Favorable monsoon environment over eastern Africa for subsequent tropical cyclogenesis of African easterly waves. *J. Atmos. Sci.*, **78**, 2911–2925, https://doi.org/10.1175/JAS-D-20-0339.1.

——, C. A. Davis, Z. L. Moon, and Q. A. Lawton, 2024: Moisture dependence of an African easterly wave within the West African Monsoon System. *J. Adv. Model. Earth Syst.*, **16**, e2023MS004070, https://doi.org/10.1029/2023MS004070.

——, E. M. Dougherty, Z. L. Moon, and C. A. Davis, 2025: Response of African easterly waves to a warming climate: A convection-permitting approach. *J. Adv. Model. Earth Syst.*, **17**, e2025MS005146, https://doi.org/10.1029/2025MS005146.

——, and Coauthors, 2026: Advancing weather and climate science in Mesoamerica and the Caribbean: A novel regional multiweek convection-permitting simulation. *Bull. Amer. Meteor. Soc.*, **107**, E836–E852, https://doi.org/10.1175/BAMS-D-25-0023.1.

Okumura, Y., and S.-P. Xie, 2004: Interaction of the Atlantic equatorial cold tongue and the African monsoon. *J. Climate*, **17**, 3589–3602, https://doi.org/10.1175/1520-0442(2004)017<3589:IOTAEC>2.0.CO;2.

Oort, A. H., 1964: On estimates of the atmospheric energy cycle. *Mon. Wea. Rev.*, **92**, 483–493, https://doi.org/10.1175/1520-0493(1964)092<0483:OEOTAE>2.3.CO;2.

Parker, D. J., and A. J. Thorpe, 1995: Conditional convective heating in a baroclinic atmosphere: A model of convective frontogenesis. *J. Atmos. Sci.*, **52**, 1699–1711, https://doi.org/10.1175/1520-0469(1995)052<1699:CCHIAB>2.0.CO;2.

Piersig, W., 1936: The cyclonic disturbances of the sub-tropical eastern North Atlantic. *Bull. Amer. Meteor. Soc.*, **25**, 2–16, https://doi.org/10.1175/1520-0477-25.1.2.

Prospero, J. M., 1968: Atmospheric dust studies on Barbados. *Bull. Amer. Meteor. Soc.*, **49**, 645–652, https://doi.org/10.1175/1520-0477-49.6.645.

——, and T. N. Carlson, 1970: Radon-222 in the North Atlantic trade winds: Its relationship to dust transport from Africa. *Science*, **167**, 974–977, https://doi.org/10.1126/science.167.3920.974.

Pytharoulis, I., and C. Thorncroft, 1999: The low-level structure of African easterly waves in 1995. *Mon. Wea. Rev.*, **127**, 2266–2280, https://doi.org/10.1175/1520-0493(1999)127<2266:TLLSOA>2.0.CO;2.

Raj, J., H. K. Bangalath, and G. Stenchikov, 2023: Future projection of the African easterly waves in a high-resolution atmospheric general circulation model. *Climate Dyn.*, **61**, 3081–3102, https://doi.org/10.1007/s00382-023-06720-y.

Rajasree, V. P. M., and Coauthors, 2023: Tropical cyclogenesis: Controlling factors and physical mechanisms. *Trop. Cyclone Res. Rev.*, **12**, 165–181, https://doi.org/10.1016/j.tcrr.2023.09.004.

Redelsperger, J.-L., C. D. Thorncroft, A. Diedhiou, T. Lebel, D. J. Parker, and J. Polcher, 2006: African monsoon multidisciplinary analysis: An international research project and field campaign. *Bull. Amer. Meteor. Soc.*, **87**, 1739–1746, https://doi.org/10.1175/BAMS-87-12-1739.

Reed, R. J., D. C. Norquist, and E. E. Recker, 1977: The structure and properties of African wave disturbances as observed during phase III of GATE. *Mon. Wea. Rev.*, **105**, 317–333, https://doi.org/10.1175/1520-0493(1977)105<0317:TSAPOA>2.0.CO;2.

——, M. D. Albright, A. J. Sammons, and P. Undén, 1988a: The role of latent heat release in explosive cyclogenesis: Three examples based on ECMWF operational forecasts. *Wea. Forecasting*, **3**, 217–229, https://doi.org/10.1175/1520-0434(1988)003<0217:TROLHR>2.0.CO;2.

——, A. Hollingsworth, W. A. Heckley, and F. Delsol, 1988b: An evaluation of the performance of the ECMWF operational system in analyzing and forecasting easterly wave disturbances over Africa and the tropical Atlantic. *Mon. Wea. Rev.*, **116**, 824–865, https://doi.org/10.1175/1520-0493(1988)116<0824:AEOTPO>2.0.CO;2.

——, E. Klinker, and A. Hollingsworth, 1988c: The structure and characteristics of African easterly wave disturbances as determined from the ECMWF operational analysis/forecast system. *Meteor. Atmos. Phys.*, **38**, 22–33, https://doi.org/10.1007/BF01029944.

Regula, H., 1936: Druckschwankungen und Tornados an der Westkuste von Afrika. *Ann. Hydrogr. Mar. Meteor.*, **64**, 107–111.

Riehl, H., 1945: Waves in the easterlies and the polar front in the tropics. Department of Meteorology, University of Chicago Miscellaneous Rep. 17, 79 pp.

Rosenthal, S. L., 1960: Some estimates of the power spectra of large-scale disturbances in low latitudes. *J. Meteor.*, **17**, 259–263, https://doi.org/10.1175/1520-0469(1960)017<0259:SEOTPS>2.0.CO;2.

Russell, J. O., A. Aiyyer, J. D. White, and W. Hannah, 2017: Revisiting the connection between African easterly waves and Atlantic tropical cyclogenesis. *Geophys. Res. Lett.*, **44**, 587–595, https://doi.org/10.1002/2016GL071236.

Russell, J. O. H., and A. Aiyyer, 2020: The potential vorticity structure and dynamics of African easterly waves. *J. Atmos. Sci.*, **77**, 871–890, https://doi.org/10.1175/JAS-D-19-0019.1.

——, ——, and J. D. White, 2020: African easterly wave dynamics in convection-permitting simulations: Rotational stratiform instability as a conceptual model. *J. Adv. Model. Earth Syst.*, **12**, e2019MS001706, https://doi.org/10.1029/2019MS001706.

Ruti, P. M., and A. Dell'Aquila, 2010: The twentieth century African easterly waves in reanalysis systems and IPCC simulations, from intra-seasonal to inter-annual variability. *Climate Dyn.*, **35**, 1099–1117, https://doi.org/10.1007/s00382-010-0894-z.

Salifou, I. T., M. Maranan, A. H. Fink, K. Kouadio, F. Yoroba, N. E. Touré, T. A. Kobea, and A. Diedhiou, 2026: Mesoscale convective system development, synoptic drivers, and forecast challenges of a catastrophic coastal rainfall event in West Africa. *Mon. Wea. Rev.*, **154**, 287–309, https://doi.org/10.1175/MWR-D-25-0021.1.

Schlueter, A., A. H. Fink, P. Knippertz, and P. Vogel, 2019: A systematic comparison of tropical waves over northern Africa. Part I: Influence on rainfall. *J. Climate*, **32**, 1501–1523, https://doi.org/10.1175/JCLI-D-18-0173.1.

Schwendike, J., 2010: Convection in an African easterly wave over West Africa and the eastern Atlantic: A model case study of Hurricane Helene (2006) and its interaction with the Saharan air layer. Ph.D. thesis, KIT Center for Climate and Environment, 200 pp., https://doi.org/10.5445/IR/1000019554.

——, and S. C. Jones, 2010: Convection in an African easterly wave over West Africa and the eastern Atlantic: A model case study of *Helene* (2006). *Quart. J. Roy. Meteor. Soc.*, **136**, 364–396, https://doi.org/10.1002/qj.566.

Semunegus, H., A. Mekonnen, and C. J. Schreck III, 2017: Characterization of convective systems and their association with African easterly waves. *Int. J. Climatol.*, **37**, 4486–4492, https://doi.org/10.1002/joc.5085.

Serra, Y. L., G. N. Kiladis, and K. I. Hodges, 2010: Tracking and mean structure of easterly waves over the intra-Americas sea. *J. Climate*, **23**, 4823–4840, https://doi.org/10.1175/2010JCLI3223.1.

Simpson, R. H., N. Frank, D. Shideler, and H. M. Johnson, 1968: Atlantic tropical disturbances, 1967. *Mon. Wea. Rev.*, **96**, 251–259, https://doi.org/10.1175/1520-0493(1968)096<0251:ATD>2.0.CO;2.

Sippel, J. A., S. A. Braun, and C.-L. Shie, 2011: Environmental influences on the strength of Tropical Storm Debby (2006). *J. Atmos. Sci.*, **68**, 2557–2581, https://doi.org/10.1175/2011JAS3648.1.

Skinner, C. B., and N. S. Diffenbaugh, 2014: Projected changes in African easterly wave intensity and track in response to greenhouse forcing. *Proc. Natl. Acad. Sci. USA*, **111**, 6882–6887, https://doi.org/10.1073/pnas.1319597111.

Sobel, A. H., J. Nilsson, and L. M. Polvani, 2001: The weak temperature gradient approximation and balanced tropical moisture waves. *J. Atmos. Sci.*, **58**, 3650–3665, https://doi.org/10.1175/1520-0469(2001)058<3650:TWTGAA>2.0.CO;2.

——, A. A. Wing, S. J. Camargo, C. M. Patricola-DiRosario, G. A. Vecchi, C.-Y. Lee, and M. K. Tippett, 2021: Tropical cyclone frequency. *Earth's Future*, **9**, e2021EF002275, https://doi.org/10.1029/2021EF002275.

Spinks, J., and Y.-L. Lin, 2015: Variability of the subtropical highs, African easterly jet and easterly wave intensities over North Africa and Arabian Peninsula in late summer. *Int. J. Climatol.*, **35**, 3540–3555, https://doi.org/10.1002/joc.4226.

Takayabu, Y. N., G. N. Kiladis, and V. Magaña, 2016: Michio Yanai and tropical waves. *Multiscale Convection-Coupled Systems in the Tropics: A Tribute to Dr. Michio Yanai, Meteor. Monogr.*, No. 56, Amer. Meteor. Soc., https://doi.org/10.1175/AMSMONOGRAPHS-D-15-0019.1.

Thorncroft, C., and K. Hodges, 2001: African easterly wave variability and its relationship to Atlantic tropical cyclone activity. *J. Climate*, **14**, 1166–1179, https://doi.org/10.1175/1520-0442(2001)014<1166:AEWVAI>2.0.CO;2.

Thorncroft, C. D., 1995: An idealized study of African easterly waves. III: More realistic basic states. *Quart. J. Roy. Meteor. Soc.*, **121**, 1589–1614, https://doi.org/10.1002/qj.49712152706.

——, and B. J. Hoskins, 1994a: An idealized study of African easterly waves. I: A linear view. *Quart. J. Roy. Meteor. Soc.*, **120**, 953–982, https://doi.org/10.1002/qj.49712051809.

——, and ——, 1994b: An idealized study of African easterly waves. II: A nonlinear view. *Quart. J. Roy. Meteor. Soc.*, **120**, 983–1015, https://doi.org/10.1002/qj.49712051810.

——, N. M. J. Hall, and G. N. Kiladis, 2008: Three-dimensional structure and dynamics of African easterly waves. Part III: Genesis. *J. Atmos. Sci.*, **65**, 3596–3607, https://doi.org/10.1175/2008JAS2575.1.

Tomassini, L., D. J. Parker, A. Stirling, C. Bain, C. Senior, and S. Milton, 2017: The interaction between moist diabatic processes and the atmospheric circulation in African easterly wave propagation. *Quart. J. Roy. Meteor. Soc.*, **143**, 3207–3227, https://doi.org/10.1002/qj.3173.

Ullrich, P. A., and C. M. Zarzycki, 2017: TempestExtremes: A framework for scale-insensitive pointwise feature tracking on unstructured grids. *Geosci. Model Dev.*, **10**, 1069–1090, https://doi.org/10.5194/gmd-10-1069-2017.

Wallace, J. M., and C.-P. Chang, 1969: Spectrum analysis of large-scale wave disturbances in the tropical lower troposphere. *J. Atmos. Sci.*, **26**, 1010–1025, https://doi.org/10.1175/1520-0469(1969)026<1010:SAOLSW>2.0.CO;2.

Wang, S.-Y., and R. R. Gillies, 2011: Observed change in Sahel rainfall, circulations, African easterly waves, and Atlantic hurricanes since 1979. *Int. J. Geophys.*, **2011**, 259529, https://doi.org/10.1155/2011/259529.

Wang, Z., 2012: Thermodynamic aspects of tropical cyclone formation. *J. Atmos. Sci.*, **69**, 2433–2451, https://doi.org/10.1175/JAS-D-11-0298.1.

——, 2018: What is the key feature of convection leading up to tropical cyclone formation? *J. Atmos. Sci.*, **75**, 1609–1629, https://doi.org/10.1175/JAS-D-17-0131.1.

——, M. T. Montgomery, and T. J. Dunkerton, 2010: Genesis of pre–Hurricane Felix (2007). Part I: The role of the easterly wave critical layer. *J. Atmos. Sci.*, **67**, 1711–1729, https://doi.org/10.1175/2009JAS3420.1.

Warner, J. L., J. Petch, C. J. Short, and C. Bain, 2023: Assessing the impact of a NWP warm-start system on model spin-up over tropical Africa. *Quart. J. Roy. Meteor. Soc.*, **149**, 621–636, https://doi.org/10.1002/qj.4429.

Wheeler, M., and G. N. Kiladis, 1999: Convectively coupled equatorial waves: Analysis of clouds and temperature in the wavenumber–frequency domain. *J. Atmos. Sci.*, **56**, 374–399, https://doi.org/10.1175/1520-0469(1999)056<0374:CCEWAO>2.0.CO;2.

Yanai, M., and M. Murakami, 1970: Spectrum analysis of symmetric and antisymmetric equatorial waves. *J. Meteor. Soc. Japan*, **48**, 331–347, https://doi.org/10.2151/jmsj1965.48.4_331.

——, T. Maruyama, T. Nitta, and Y. Hayashi, 1968: Power spectra of large-scale disturbances over the tropical Pacific. *J. Meteor.

Soc. Japan, **46**, 308–323, https://doi.org/10.2151/jmsj1965.46.4_308.

Yang, G.-Y., J. Methven, S. Woolnough, K. Hodges, and B. Hoskins, 2018: Linking African easterly wave activity with equatorial waves and the influence of Rossby waves from the Southern Hemisphere. *J. Atmos. Sci.*, **75**, 1783–1809, https://doi.org/10.1175/JAS-D-17-0184.1.

Zawislak, J., and E. J. Zipser, 2014: A multisatellite investigation of the convective properties of developing and nondeveloping tropical disturbances. *Mon. Wea. Rev.*, **142**, 4624–4645, https://doi.org/10.1175/MWR-D-14-00028.1.

——, E. Nowottnick, and A. Nehrir, 2022: Convective processes experiment—Cabo Verde (CPEX-CV) field campaign collection. NASA EOSDIS Global Hydrometeorology Resource Center Distributed Active Archive Center, accessed 15 May 2026, https://doi.org/10.5067/CPEXCV/DATA101.

Zhang, C., 2005: Madden–Julian Oscillation. *Rev. Geophys.*, **43**, RG2003, https://doi.org/10.1029/2004RG000158.

Zipser, E. J., and Coauthors, 2009: The Saharan air layer and the fate of African easterly waves—NASA's AMMA field study of tropical cyclogenesis. *Bull. Amer. Meteor. Soc.*, **90**, 1137–1156, https://doi.org/10.1175/2009BAMS2728.1.